Microwave Journal

eBook

Autonomous Driving Design Technology

May 2019

SPONSORED BY ROGERS CORPORATION

Table of Contents

Introduction

Autonomous Driving Design Technology

As noted in the first article of this eBook, the global automotive industry is going through a period of wide-ranging and transformative changes with the shift in the consumer behavior as well as increasing implementation of stringent environmental regulations and autonomous vehicles are changing urban transportation beyond recognition in the next few years. BIS Research analysis estimates the global autonomous vehicle market was valued at 6.6 million units in 2017 and is expected to reach 67.5 million units by 2028, registering a CAGR of 20.78% between 2018 and 2028.

We have seen autonomous vehicle announcements from the traditional cars companies, new car companies such as Tesla, new startups like Waymo and ride sharing companies like Uber as everyone is trying to be first to market. A critical sensor in the autonomous suite is the radar module currently being used for ADAS applications in many cars. These sensors are becoming more capable for autonomy with wider bandwidth signals for better resolution, improved software/processing for 3D and micro Doppler imaging, and more integrated to lower size/cost.

With this improved performance comes many challenges in the area of design and testing. This eBook addresses many of those challenges with articles covering the effects of materials on 77 GHz radar modules, interference challenges in urban environments, testing challenges, and PCB materials solutions to the thermal and high frequency effects.

We hope these articles will solve some of the technical challenges you are facing with your high frequency designs and offers solutions to designing and testing radar modules. We thank Rogers Corporation for sponsoring this eBook to bring this content to you for free.

Pat Hindle, Microwave Journal *Editor*

Global Autonomous Vehicle Market to Grow at a CAGR of 20.78% from 2018-2028

Market Report from Report Linker

The global automotive industry is going through a period of wide-ranging and transformative changes with the shift in the consumer behavior as well as increasing implementation of stringent environmental regulations. Factors such as rising safety and security concerns, increasing demand for reliable transportation system, and advent of revolutionary trends, such as transition from car ownership to "Mobility as a Service" (MaaS), are expected to increase the demand for autonomous vehicles.

Autonomous vehicles are the key to changing urban transportation beyond recognition in the next few years.There are both traditional OEMs and new vehicle developers who are working in this ecosystem to improve and introduce fully-autonomous vehicles on the road. These vehicles will have advanced features from traditional vehicles and improve the driving experience for passengers. The Society of Automotive Engineers International (SAE) has defined six levels of automation to classify a system's sophistication, ranking from 0 to 5.

LEVEL 0: NO AUTOMATION

In this level, the driver is in control of the entire vehicle and all aspects of driving are entirely manually controlled. Example of such a vehicle is 2018 KIA Rio, among others.

LEVEL 1: DRIVER ASSISTANCE

In this level, the vehicle system can assist with some functions such as controlling the steering or the vehicle speed.The driver handles a majority of the vehicle functions. Features such as adaptive cruise control or lane keeping are part of this level of automation.

LEVEL 2: PARTIAL AUTOMATION

In this level, the vehicle system is able to control the braking, steering, or acceleration of the vehicle.These features can be applied together and the coordination between two or more of these assist technologies helps a vehicle to be of Level 2 status. A driver is there during all times to actively monitor the vehicle's progress and be ready to intervene at any time. Most vehicles in 2018 have these features of Level 2 such as GM Super Cruise, Mercedes-Benz Distronic Plus, Tesla Autopilot, Nissan ProPilot Assist, and Volvo Pilot Assist, among others.

LEVEL 3: CONDITIONAL AUTOMATION

In this level, the vehicle system is able to detect the environment around the vehicle using sensors such as LiDARs and make informed decisions for the vehicle such as overtaking a slower moving vehicle in front of it.The vehicle system is able to manage most aspects of driving, including monitoring the environment. The system prompts the driver to intervene when it encounters a scenario it can't navigate. Audi Traffic Jam Assist is the only commercialized level 3 auto pilot system developed by Audi for Audi A8.

LEVEL 4: HIGH AUTOMATION

In this level, the vehicle can operate without human intervention but only in certain conditions. There is an option to manually override the vehicle system functions.

LEVEL 5: FULL AUTOMATION

In this level, the vehicles can operate as driverless vehicles in any road conditions. These vehicles are being

developed to be used as robo-taxis, such as Waymo, among others.

The global autonomous vehicle market has witnessed several strategic and technological developments in the past few years, undertaken by the different market players to attain their respective market shares in this emerging domain. Some of the strategies covered in this section are product launches and developments, business expansions, and partnerships/collaborations/ joint venture. The preferred strategy for the companies have been product launches & developments in order to strengthen their position in the global autonomous vehicle market.

According to BIS Research analysis, the global autonomous vehicle market was valued at 6.6 million units in 2017 and is expected to reach 67.5 million units by 2028, registering a CAGR of 20.78% between 2018 and 2028. North America dominated the global autonomous vehicle market in 2018, whereas, Rest-of-the-World is expected to have the highest growth rate during the forecast period 2018-2023.

The key market players in the global autonomous vehicle market are Audi AG, BMW Group, Daimler AG, FCA Italy S.p.A., Ford Motor Company, General Motor Company, Nissan Motor Corporation, Tesla Inc., Toyota Motor Corporation, Volkswagen AG, Volvo Group, Waymo LLC, and Zoox Inc.

Evaluating 77 to 79 GHz Automotive Radar Radome Emblems

Steffen Heuel, Tobias Köppel and Sherif Ahmed
Rohde & Schwarz, Munich, Germany

Advanced driver assistance systems (ADAS) in cars assist the driver and increase road safety, and these systems are widely deployed in many modern vehicles and car types. Currently, autonomous driving is a major focus of the automotive industry, and R&D institutes are making headlines with fully automated cars driving hands-off along the highway—even in cities with dense traffic. It is certain that autonomous driving will become reality in the near future.

Camera, LiDAR and radar sensors are key enabling technologies in this area. Millions of automotive radars are produced every year, and car manufacturers are starting to deploy them as standard equipment in all higher-class cars. Today, automotive radar sensors are mainly used to increase driving comfort and prevent crashes. Most automotive radar sensors that enable adaptive cruise control (ACC) operate in the conventional 76 to 77 GHz frequency range to sense other cars and objects far ahead. Advanced radar capabilities, however, demand larger bandwidths, with coverage up to 81 GHz to enable 360 degree radar vision around the vehicle. This is required for ADAS functions such as lane change assistance and blind spot detection, where high resolution and a wide operating angle are essential. Additionally, extending the automotive frequency band to 81 GHz helps mitigate interference. Altogether, this puts pressure on radar system integration to be functional across a wider frequency band than in the past.

▲ **Fig.1 Radar mounted behind the front emblem, which is a radome.**

Automotive radars must be masked by a cover, known as a radome, which is constructed from a transparent RF material. Radomes can be an emblem or a car bumper, with the radar behind it as illustrated in ***Figure 1***. Although an emblem may be underestimated and dismissed as a simple plastic cover, it is actually a sophisticated RF element that often degrades radar detection range and accuracy. Emblems need to satisfy the requirements of aesthetic appearance, often including the 3D shape of the car logo. However, this is usually in conflict with the RF performance needed for 76 to 81 GHz operation. On the other hand, car bumpers are typically coated with metallic paint, which is, of course, critical for the automotive radar frequencies. So it becomes essential to validate the material characteristics and examine their influence on the radar sensors. Considering the criticality of the applications where radar sensors are deployed, uncertainties are unacceptable. Consequently, engineers and manufacturers need new measurement capabilities to evaluate the effect of em-

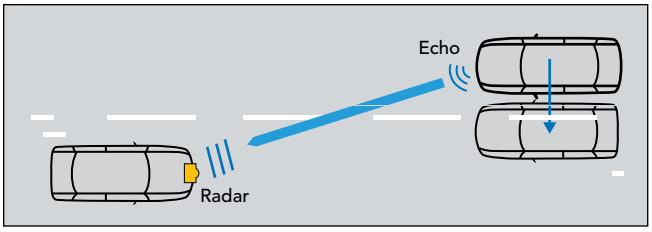

▲ **Fig. 2 At 100 m range, an azimuth error of 1° causes a target location error of 1.75 m.**

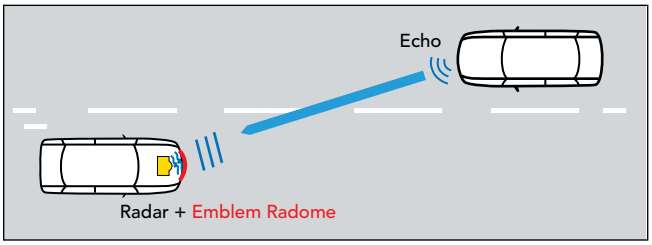

▲ **Fig. 3 Inhomogeneous radome material causes planar wave distortion and attenuation, leading to azimuth errors and reduced detection performance.**

blem radomes and bumpers on radar performance. This article explains a novel radome measurement method and discusses the radome's influence on the accuracy of the angle of detection with advanced radars.

RADOME INFLUENCES

Automotive radar sensors transmit radio signals at 24 and 77 to 79 GHz. They mainly use frequency modulated continuous wave signals that have the advantages of low power, no "blind" range and low receiver bandwidth, meaning they can be manufactured more cost effectively than pulsed radar systems. The transmitted radio signals are reflected by other objects. Due to the propagation delay and Doppler frequency shift, the radar sensor can measure and resolve range and radial velocity for multi-target situations. Depending on the properties of the antenna array, it is also possible to measure and resolve the azimuth and elevation angles. After the detection process and tracking, signal processing generates a target list that contains values such as the positions and velocities of objects and estimates of type. This list is passed to the vehicle's electronic control unit (ECU), where it is further processed to deliver real-time decisions for vehicle maneuvers. The accuracy and reliability of this data is extremely important for the safety of the vehicle and its passengers.

The accuracy of a radar depends on many factors, such as the hardware components, software processing and the radar echo signal itself. The parameters of signal echoes with lower signal-to-noise ratio (SNR) can be measured less accurately than signals with high SNR. The effects of multipath propagation and distortion due to radomes greatly impact measurement accuracy. Inaccuracies in the azimuth measurement cause the target to appear misplaced. This is shown in ***Figure 2***, illustrating that an angular measurement error of only 1 degree at the radar sensor causes a target at 100 m range to appear misplaced by 1.75 m in azimuth. The target will be interpreted as located in the neighboring lane. In practice, angular accuracy for such far distances must be significantly less than 1 degree for reliable operation.

For a modern radar sensor with an antenna array receiver front-end, the azimuth (and sometimes the elevation angle) is estimated from phase and amplitude information using digital beamforming on the receive side. To get the best azimuth measurement accuracy, every radar sensor needs to be adjusted. The following procedure is typical for radar calibration. First, the radar sensor is mounted on a turntable in an anechoic chamber. A corner reflector in the far field at a known distance is commonly used as a reference target. The radar pattern is then measured and flashed into the radar sensor's memory. Later, this information is used by the detection algorithm. This ensures high azimuth measurement accuracy when the radar sensor completes production. The car manufacturer integrates this calibrated radar sensor into the car, often behind an emblem or the bumper, where the radome material influences the RF attenuation. The radome's transmission loss increases the two-way attenuation of the radar signal, which reduces the maximum detection range of the radar. The power level of a transmitted radar signal is reduced by the range, R, to the target and by R^4 on the return. For a 77 GHz radar system with 3 W output power, 25 dBi antenna gain, a target with a 10 m^2 radar cross-section and a minimum detectable signal of -90 dBm, the maximum range would be 109.4 m, according to the range equation. If the radome has 3 dB two-way attenuation, the maximum range of the same radar measuring the same target would decrease to 92.1 m. That is approximately 16 percent less range.

It is not only material attenuation that has a great impact. The material reflectivity and homogeneity also play important roles. Reflections and RF mismatch of the material cause direct signal reflections in close range to the radar. The signals are received and down-converted in the receiver chain, reducing the radar's detection sensitivity. Many car manufacturers try to mitigate this effect by tilting the radomes—not only for design reasons—to reflect the transmitted radar signal somewhere other than directly back into the receiver front-end. This solution, of course, has mechanical limitations, not to mention the expected loss of RF energy from these parasitic reflections. Another problem comes from material inhomogeneities that disturb the echo signal wavefront used to estimate the azimuth value. Inhomogeneous material distorts the wavefront, which results in less accurate angular measurements.

The radar sensor calibration is no longer sufficient, since the previously calibrated radar can be mounted behind any indeterminate radome from a different manufacturer (see ***Figure 3***).

MATERIAL CHARACTERIZATION

Radome manufacturers typically test their units with a known or "golden" radar. For this test, several corner reflectors are mounted in front of the radar at predetermined ranges and azimuth positions (see ***Figure 4***). A differential measurement is conducted with and without the radome, and these measurements are compared. For the radome to pass the test, the range/azimuth positions and echo signal levels must be within defined

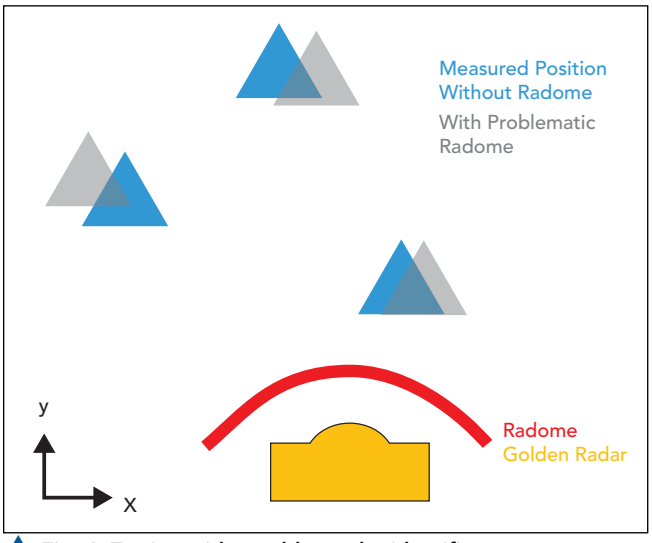

Fig. 4 Testing with a golden radar identifies some errors and signal degradation caused by the radome.

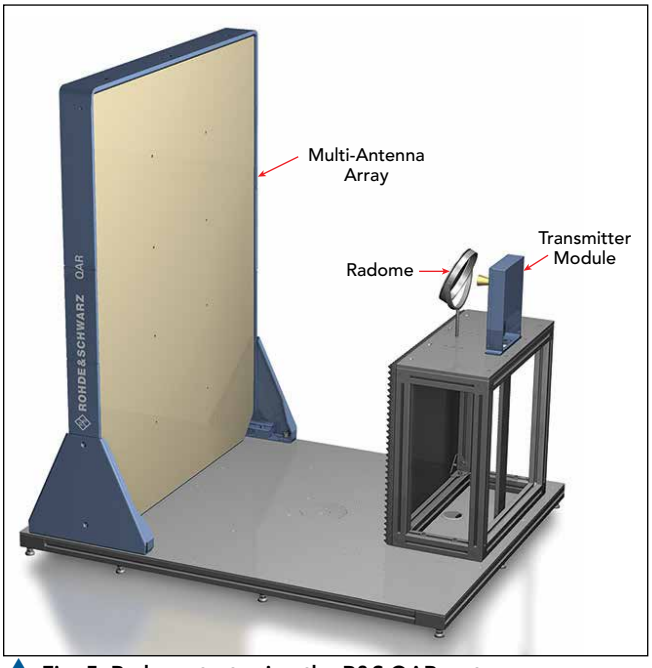

Fig. 5 Radome test using the R&S QAR system.

limits. However, this approach only tests certain azimuth angles and does not account for possible inhomogeneity or blind spots.

Another measurement method relies on a functional test. The radar sensor with the radome is mounted on a turntable and a corner reflector is placed in front of them. By turning the complete unit, every azimuth and elevation angle can be measured and compared to the radar-only standard. This method is as accurate as the positioning of the turntable; however, the test takes a long time and is not feasible for production tests.

Instead of testing transparent radar material with a golden device, a proposed novel measurement method combines a transmission measurement with three-dimensional, high resolution radar imaging in the 77 to 79 GHz frequency band used by the radar itself. This is done using the R&S QAR system (see ***Figure 5***). A

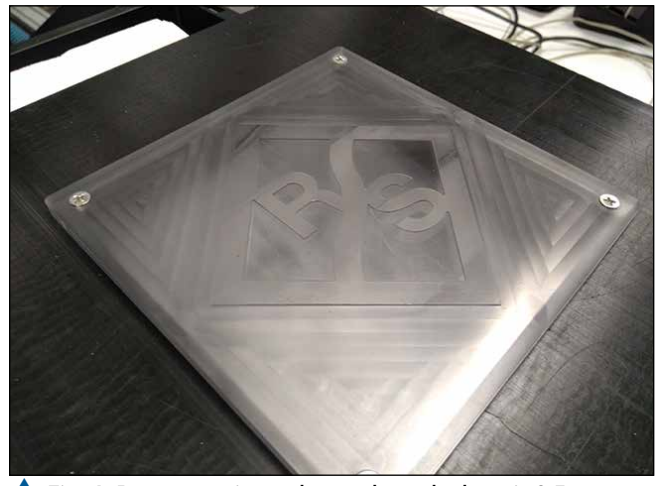

Fig. 6 Demonstration radome where the logo is 0.5 mm thicker than the radome material, causing an impedance mismatch at 77 GHz.

multi-antenna array consisting of several hundred transmit and receive antennas operating from 75 to 82 GHz is used. This measurement system can measure the range, azimuth and elevation with millimeter resolution. It operates in the same frequency band as the automotive radar and "sees" what the automotive radar would see if it also had hundreds of transmit and receive antennas. Thanks to the large aperture, the resolution of the test system is much higher than that of the automotive radar, and it can visualize the measurement as an image. The radome is placed in front of the test system, which performs a two-stage measurement.

Reflectivity

First, a reflectivity measurement determines the amount of energy reflected by the radome material; this is energy that does not pass through the radome and contributes to performance degradation. Reflected signals decrease the performance of the radar and can even interfere with the received signals. Areas with high reflectivity can have various causes, such as material defects, air gaps, undesired interaction between layers of material, excessive amounts of certain materials or foreign objects. The measurement method achieves a spatially resolved reflectivity measurement for a radome by linking the information collected by the distributed, coherent transmit and receive antennas. The receive signals are gated and processed for all receive antennas, which results in a high resolution 3D radar image. The resulting mmWave image enables intuitive as well as quantitative evaluation of the radome's reflection behavior.

To illustrate the approach, a radome was manufactured where the R&S logo was milled with different thickness, as shown in ***Figure 6***. The high resolution radar image in ***Figure 7a*** visualizes what an automotive radar sensor would perceive when covered by this radome. The color scale shows the reflectivity, where the dark color indicates minimal reflectivity and bright high reflectivity. Metal, which cannot be penetrated by automotive radar signals, appears as white (e.g., the screws in the four corners). The radome image indicates high reflectivity and the inhomogeneity of the logo, showing

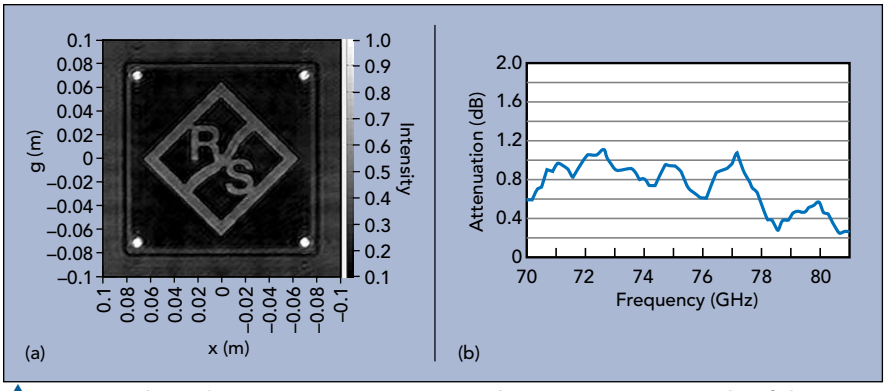

▲ **Fig. 7 High-resolution mmWave image (a) and one-way attenuation (b) of the demonstration radome.**

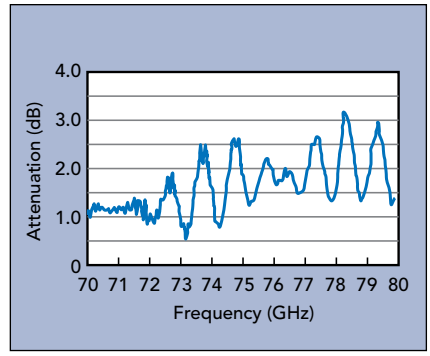

▲ **Fig. 8 Transmission measurement of a commercial, multi-layer radome with a complex 3D design.**

the increased thickness of 0.5 mm in the logo area is sufficient to cause major disturbances in radar performance on the street. In this example, calculating the mean reflectivity in the middle area, where the radar sensor is usually mounted, yields approximately -11 dB with a standard deviation of -17.7 dB. In many practical cases, this reflection is too high to maintain acceptable radar operation. In practice, the expected reflectivity depends on the sensitivity of the radar and the maximum detection distance to be covered.

Transmission

In a second test, the frequency matching and attenuation of the radome material is measured. A transmitter module is located behind the radome on the table. The transmitter uses a frequency sweep to cover a selected frequency span. This allows the radome's transmission frequency response to be measured. The frequency response delivers detailed information about the RF matching of the radome at the frequencies intended for radar operation. It is independent of the signal waveform used by the radar, which facilitates the testability and optimization of the radome itself.

The measured one-way attenuation versus frequency of the radome is shown in ***Figure 7b***. Since automotive radars operate in the 76 to 81 GHz band, attenuation should be low across this range. Depending on the thickness of the material, its air gaps and RF matching, a good radome should maintain low attenuation across the desired frequencies. The logo example shows 0.64 dB one-way attenuation with better matching at 79 than at 76 GHz. A more sophisticated example for commercial radomes with a 3D design typically results in a transmission measurement, as shown in ***Figure 8***. This radome would have various performance issues:

- Frequency matching is incorrectly placed around 71 instead of 76 GHz, which is often caused by increased thickness of some radome layers
- Significant increase in the standing wave ratio within the 79 GHz band, which identifies high reflections at the radome boundaries and a strong interference phenomenon
- Overall one-way attenuation is relatively high, which results in a significant reduction in the detection range.

SUMMARY

Researchers are already driving autonomous cars on the highway and in city traffic. Due to the all-weather capability of radar sensors, their reliability and their price, these sensors are essential in automotive applications. Integration behind bumpers and emblems also makes them attractive for car designers. Without high-quality radomes, objects with low radar cross-sections, such as pedestrians, will likely be undetected and may even appear at erroneous azimuth angles. Even larger objects at far distances may be incorrectly identified and measured at different positions when the radar signal is distorted by the inhomogeneous radome material.

This article presented a novel measurement method that can be applied for any kind of automotive radome operating in the 75 to 82 GHz band, such as the ones used in emblems, bumpers or front grills that cover automotive radar sensors. Using a massive multistatic array, within a few seconds this method measures and calculates the mean reflectivity and standard deviation of a defined area (homogeneity) and the transmission loss over the complete frequency range. The visualization of the results as an image assists radome designers and R&D labs, while determining a pass/fail result based on the radome's RF performance significantly speeds production, especially at end-of-line testing.n

Watch a video demo of the Rohde & Schwarz QAR system

Editor's Note: Whether for automotive radar or 5G, mmWave systems will require OTA testing to characterize and verify system performance. So we have included this article on 5G OTA testing, as the principles are applicable to autonomous driving systems.

Test & Measurement Industry Tackles 5G Over-the-Air Testing

Pat Hindle
Microwave Journal *Editor*

With the full approval of Release 15 by the 3GPP in June 2018, 5G commercial networks were quickly launched in the U.S. (Verizon and AT&T) and South Korea (KT, LG UPlus and SK Telecom) by the end of the year. In 2019, the industry will see increased activity with many 5G launches and a major shift in emphasis from LTE to 5G networks. Since 5G testing standards are still not completely defined, base station and handset manufacturers, wireless carriers and regulators have to come together quickly around the world and agree on how to install, verify and maintain commercial 5G networks. At this critical point in time, Microwave Journal *reached out to nine leading test & measurement companies in the industry and compiled their information about the challenges and solutions currently available in the area of 5G over-the-air (OTA) testing. The companies included Anritsu, EMITE, ETS-Lindgren, Keysight, MVG, National Instruments (NI), NSI-MI, Rohde & Schwarz (R&S) and Boonton, Noisecom.*

5G TEST CHALLENGES

Anritsu outlined the primary challenge due to the fundamental differences in the technology used in 5G testing—like mmWave frequencies, massive arrays of antennas, beamforming and dynamic physical layer attributes—so trying to apply LTE test methods to 5G networks will not work. Countries in different regions of the world are using different frequency bands for 5G deployments, and in addition to showing compliance with the 3GPP 5G New Radio (NR) standard, many countries require compliance with local government regulations.

R&S wrote in a recent *Microwave Journal* article that 5G deployment will rely on the performance of highly integrated solutions combining the modem, RF front-end and antenna. The challenge is to define new methods and setups for performance evaluation, as RF test ports tend to disappear and beam steering technologies require system-level testing. In this context, both antenna and transceiver performance criteria must be measured OTA: effective isotropic radiated power (EIRP), total radiated power (TRP), effective isotropic sensitivity (EIS), total isotropic sensitivity (TIS), error vector magnitude (EVM), adjacent channel leakage ratio (ACLR) and spectrum emission mask (SEM) are some of the critical measurements needed.

R&S continued with the point that assessing these OTA raises the critical question of the required measurement distance. Antenna characteristics are usually measured in the far field (see ***Figure 1***). Using direct far-field probing and applying the Fraunhofer distance

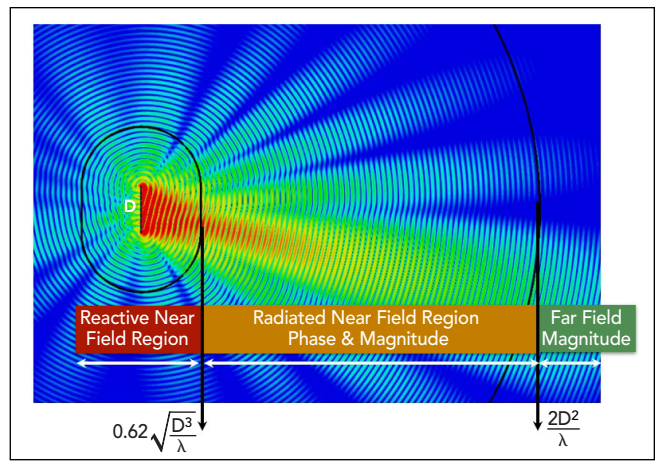

Fig. 1 R&S provided antenna radiation pattern in the near-field, far-field, and Fraunhofer distances.

criterion ($R = 2D^2/\lambda$), a 75 cm massive MIMO device under test (DUT) radiating at 2.4 GHz should be evaluated in a chamber with at least 9 m range length. Even a 15 cm smartphone transmitting at 43.5 GHz needs a 6.5 m testing distance. This distance is required to create a region encompassing the DUT, where the impinging field is as uniform as possible and approaches a plane wave with phase deviation below 22.5 degrees, known as the quiet zone.

One way to overcome the space constraint of a big chamber is by using a reflector that projects the incoming spherical wave front to a plane wave due to the re-

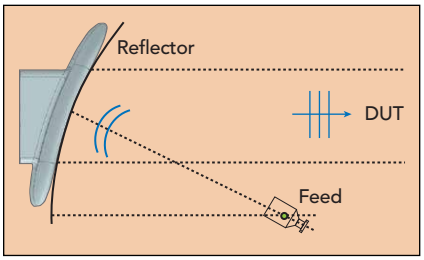

Fig. 2 Diagram of how a compact antenna test range operates.

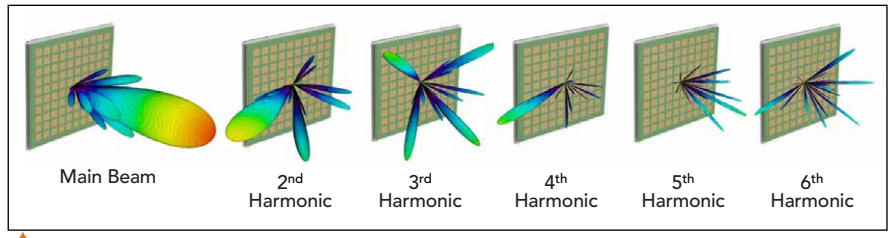

Fig. 3 ETS-Lindgren provided radiation pattern for a 28 GHz phased array showing the main beam to the left and the first through sixth harmonic radiation patterns going left to right.

flector's parabolic shape. Using such a reflector is a well-known method for mmWave OTA setups and is called a compact antenna test range (CATR). The principal is shown in ***Figure 2***.

Anritsu said a key companion to EIRP is gated sweep. With a gated sweep, the user can define which portion of the 5G transmission to measure. This is important because 5G NR signals can be configured through the slot configuration parameter in 55 different TDD Tx/Rx ratios in a 10 ms frame. By gating only the subframe or symbol of interest, the user can ensure that only the RF of the downlink is measured. This will give a more true representation of the RF energy being radiated into the atmosphere.

ETS-Lindgren and Anritsu both noted that significant changes are needed for meaningful EMC tests on 5G devices. TRP is a common measurement required by regulatory standards to ensure radios are not transmitting too much power. Because the signal is transmitted from one isotropic transmitter that is radiating energy evenly across an entire sector in LTE, it is easy to make a measurement on the total power at the radio and determine if the atmospheric energy is within safe limits. ETS-Lindgren stressed the challenge with beamforming as shown in ***Figure 3***; there is no easy way to measure the energy at any single point and know how much power is being transmitted into space since it is directional. With side lobes and back lobes, the only way to measure the TRP is to integrate the power in a 360 degree sphere around the entire antenna. While this can be done, it can be expensive and time consuming.

Anritsu commented that as the industry starts to converge on installation and maintenance best practices, the next challenge will be defining procedures and finding equipment that will make the test as accurate, efficient and affordable as possible. This will require test vendors to react quickly to test needs and be ready with new generation hardware that can meet the challenge.

OTA TEST METHODS

Keysight explained the test methods well, stating that when defining an OTA test strategy, it is important to have a good understanding of what will be tested, how it should be tested and what are the appropriate test methods for the different test cases. In the consumer market, testing will be done on modems, antennas, subsystems and fully assembled end-user devices. Base stations will follow a similar testing workflow. A typical testing cycle starts from R&D through conformance and device acceptance testing.

Typically, tests can be categorized into conformance and performance tests. Conformance tests are mandatory tests that need to be completed to release a device. Conformance tests are a key requirement and involve connecting a device to a wireless test system and performing the required 3GPP tests:

- RF transmission and reception performance—minimum level of signal quality.
- Demodulation—data throughput performance.
- Radio resource management (RRM)—initial access, handover and mobility.
- Signaling—upper layer signaling procedures.

Keysight stated that modem chipsets, antennas, base stations and integrated devices will require a mix of conducted and OTA tests. Most frequency range 1 (FR1: 450 MHz to 7.125 GHz) tests will be done using conducted measurements, while 3GPP has defined all frequency range 2 (FR2: 24.25 to 52.6 GHz) conformance tests to be done using OTA test methods.

To date, there are three OTA test methods approved by 3GPP, according to Keysight:

- **Direct Far Field (DFF):** The measurement antenna is placed in the far field. The far-field or Fraunhofer distance begins at $2D^2/\lambda$, where D is the maximum diameter of the radiating elements and λ is the wavelength. This is where the angular field distribution stops evolving. The direct far-field method can perform the most comprehensive tests, measuring multiple signals, but can also result in a longer test range at mmWave frequencies.
- **Indirect Far Field (IFF):** A far-field environment is created using a physical transformation, typically involving a parabolic reflector to collimate the signals transmitted by the probe antenna. This method is limited to measuring a single signal angle of arrival/departure but provides a much shorter distance with less path loss. This test method is accomplished using a CATR.
- **Near Field to Far Field Transformation (NFTF):** Phase and amplitude of the electrical field are sampled in the radiated near-field region, and the far-field pattern is computed. This method is also limited to a single line-of-sight transceiver measurement.

According to R&S, as of early January 2019, 3GPP specified a number of transmitter and receiver tests in the 3GPP TS38.521-3, which is the NR User Equipment (UE) conformance specification for radio transmission and reception where "–3" refers to part 3 and means FR1 and FR2 interworking operation with LTE, basically Non-Standalone (NSA) sub-6 GHz as well as NSA mmWave.

For mmWave, testing becomes more difficult since everything will need to be tested OTA and a black box approach has to be assumed. This means that achiev-

TABLE 1

HIGH LEVEL SUMMARY OF FIDELITY AND APPLICABILITY OF 5G TEST ENVIRONMENTS (CREDIT: NSI-MI)

	AUT Size	FF	DFF	IFF	NFTF
RF Testing	Small UEs				Tx only
	Large UEs				Tx only
	gNodeBs				Tx only
Demod Testing	Small UEs				
	Large UEs				
	gNodeBs				
RRM Testing	Small UEs				
	Large UEs				
	gNodeBs				

able measurement uncertainties (MU) and test tolerances (TT) will need to be much wider than in sub-6 GHz FR1 conducted testing. It is an ongoing discussion in 3GPP which MUs are acceptable and what TT to use for FR2. Until this is fixed by 3GPP, spec compliant RF conformance tests for FR2 are not practical.

For Standalone (SA) deployment scenarios, the matching 38.521 parts 1 (sub-6 GHz) and 2 (mmWave) are more advanced, even though the first 5G NR deployments early this year will be NSA. On top of this, the specifications for performance tests (38.521-4) and RRM test requirements (38.533) are not yet ready for NSA.

Table 1, created by NSI-MI, summarizes the applicability of the test environments to different types of testing and different antenna sizes. Colors indicate quality of the solution in terms of SNR, utility, cost, etc.

EMITE said there is no single OTA test method capable of providing the answers to all of the problems and challenges we have today. Therefore, industry will need to adopt a variety of methods. Some companies have shown that there are benefits to rich isotropic systems for obtaining some key performance parameters, while directionality is needed to address the evaluation of other 5G features. Simultaneously testing at both near- and far-field distances, low and high frequencies, large and small form factors may also be needed.

ETS-Lindgren added that engineers often ask if a single do-it-all chamber for 5G OTA, EMC and cable replacement tests could be designed. They find there are too many compromises each method would impose on the others to make this a cost effective approach. Measurement uncertainty requirements drive optimization in different directions for each type of test. Consider the additional absorber and measurement antennas that would need to be moved in and out of a traditional 3 m EMC chamber quiet zone to transition between EMC and far-field OTA requirements. The transition time and costs associated with a do-it-all test chamber will mostly outweigh the benefits.

OTA PRODUCT OFFERINGS

Here are some of the OTA solutions being offered by these leading test & measurement suppliers:

Fig. 4 Anritsu's Field Master™ Pro MS2090A handheld solution.

Fig. 5 EMITE's F-Series 200 MHz to 110 GHz hybrid Anechoic-reverberation chambers.

Anritsu's New Solution

With the launch of the Field Master™ Pro MS2090A at MWC Barcelona 2019 in February, Anritsu introduces the first field portable instrument with continuous frequency coverage for sub-3 GHz, sub-6 GHz and mmWave 5GNR measurements (see ***Figure 4***). The Field Master Pro MS2090A has been developed in close cooperation with all leading 5G base station manufacturers, as well as being used to install the first commercial 5GNR networks. This should have a significant impact on the testing market to have this capability in a handheld unit.

The key features of the Field Master Pro MS2090A are:

- Continuous frequency coverage from 9 kHz to 9, 14, 20, 32, 44 or 54 GHz.
- 100 MHz analysis bandwidth for current 5G deployments.
- 5G NR demodulation capabilities.
- RTSA for interference hunting.
- Built-in EIRP and gated sweep for transmission testing.
- 10.1 in. multi-touch screen user interface.

EMITE Solutions

For a small company in this space, EMITE offers a broad range of solutions. The EMITE PT-Series is a small

reverberation chamber which serves as a simple go, no-go mmWave SISO OTA test and some non-signaling production OTA tests for up to eight simultaneous DUTs of up to 15 cm.

Their E-Series is a medium-size reverberation chamber capable of providing fully-automated 5G OTA testing of some isotropic key performance indicators, as well as latency and throughput. The E-Series chambers can easily accommodate many carriers with 4G and 5G technologies, with up to 8×8 MIMO, and can make use of channel emulators for 5G channel modeling. A unique solution from EMITE, these can also be cascaded to test massive MIMO and E2E OTA tests, representing a first step into 5G OTA signaling testing.

Fig. 6 EMITE H-Series 600 MHz to 110 GHz small anechoic chamber including climatic enclosure.

Fig. 7 ETS-Lindgren's table top AMS-5700 OTA test chamber.

TABLE 2

KEYSIGHT'S RANGE OTA TESTING SOLUTIONS

	UE RF Tx	UE RF Rx	DEMOD	RMM	Protocol Signaling
Direct Far-Field (DFF)	✓	✓	✓	✓	✓
Simplified DFF	✓	✓	✓	✓	✓
Indirect Far-Field (IFF)	✓	✓	✓	✓	✓
Near-Field with Transformation (NFTF)					
Near-Field Without Transformation (NFWOT)			✓		

Their F-Series is a hybrid reverberation-anechoic chamber capable of providing a blend of both worlds (see ***Figure 5***). The RC mode provides easy, fully-automated overnight testing of 4G and 5G OTA while the AC mode incorporates all 3GPP-permitted OTA test methods (IFF, NFTF and DFF) for DUTs of up to 1.5 m.

The H-Series is a small anechoic chamber intended to simultaneously test FR1 and FR2 frequency combinations using a combined CATR, spherical near-field (SNF) and DFF test system with the only climatic foam enclosure in the market for testing wireless OTA under both temperature and humidity conditions (see ***Figure 6***). Temperature range from −40°C to 90°C with fluctuation of about ±0.5°C and heating and cooling change rates of 2°C to 4.5°C per minute, and humidity range from 10 to 98 percent relative humidity with fluctuations of ±0.5 to ±3 percent relative humidity are available.

ETS-Lindgren Solutions

Labs with current ETS-Lindgren OTA systems or those manufactured by others will be pleased to know that an upgrade package for 5G testing in the sub-6 GHz, FR1 band is available. This upgrade is economical and backward compatible, providing a three generation OTA system covering 5G, 4G and 3G, if so equipped.

For 5G FR2 mmWave OTA, ETS-Lindgren offers the AMS-5700 series of OTA test chambers (see ***Figure 7***). The AMS-5700 series is highly flexible, offering one system serving multiple projects and use cases. The 5700 series offers direct and indirect far-field configurations covering any array size up to 60 cm. The AMS-5703 is designed with a large quiet zone and unique positioning system to accommodate future CTIA phantom test requirements.

ETS-Lindgren also offers custom solutions: one recent ETS-Lindgren project enabled end-to-end data throughput, MIMO and beam steering performance to be measured on gNBs linked to moving UEs. Another complex automotive project provided vehicle to everything (V2X) measurement and optimization results from dozens of antennas and sensors integrated in an autonomous vehicle.

Keysight Solutions

Keysight offers a portfolio of OTA solutions based on the workflow from R&D to device acceptance. A typical solution consists of measurement software, a network emulator to emulate a 5G gNB and a channel emulator to emulate the radio conditions. For FR2, these solutions include OTA measurement systems, typically adding RF enclosures, probe and link antennas, different DUT positioners and associated control software. Keysight's offerings address the different test approaches and the varying needs for modems, antennas, integrated devices and base stations. OTA tests are required from R&D through design validation, protocol and RF/RMM conformance testing and device acceptance testing. Keysight supports the wide range of solutions shown in ***Table 2***.

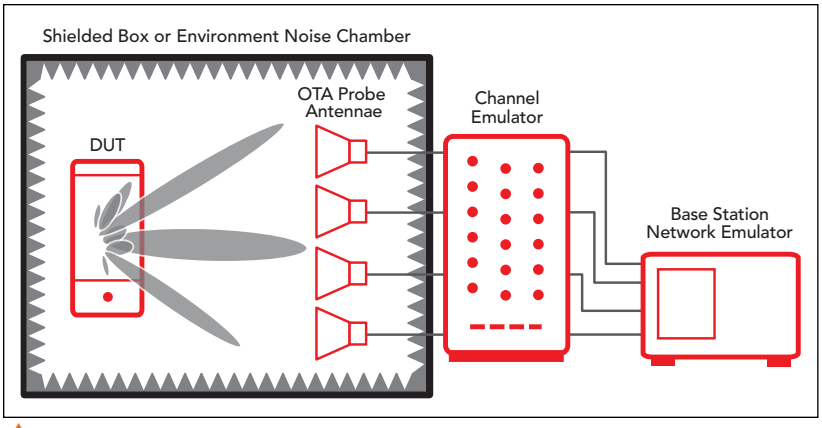

▲ **Fig. 8 Keysight's multiprobe anechoic chambers (MPAC) solution.**

Keysight has CATR solutions that offer IFF measurements for RF, RF parametric testing and antenna pattern measurements, well suited for testing antennas, phones, phablets, tablets, laptops and small 5G gNBs. To test devices under real world operating conditions, a solution needs to emulate different directions of arrival of the 5G signal, i.e., emulating the spatial characteristics of the environment. For this, Keysight models signal from the base station (gNB) to the device. Their multi-probe anechoic chamber solutions are good for understanding how a device operates in the spatial environment with multiple simultaneous radiated beam angles (see ***Figure 8***). This solution utilizes the Keysight UXM 5G Wireless Testset, PROPSIM F64 channel emulator and performance network analyzers for testing the device under real world conditions for different key performance indicators like throughput, handover, etc.

MVG Solutions

MVG offers multi-probe systems based on rapid sampling, using probe arrays of the radiated near field in amplitude and phase on a closed surface around the device. The far-field performance of the device is determined from near-field to far-field transformation. The exact knowledge of the amplitude and phase of the radiating device gives access to important investigative features on the device behavior through post processing.

As the electrical size of devices and systems at 5G frequencies increase, the sampling required for exhaustive testing of the devices becomes a burden to the users, as the testing time increases. The multi-probe systems from MVG enable much faster testing than traditional single probe systems allowing users to fully characterize their devices within much more reasonable times, enabling in-the-loop research and development activities (see ***Figure 9***).

When integrating antennas on larger electrical devices, as is the case for the small arrays integrated on handheld 5G devices, the coupling phenomenon between antennas can significantly alter device performance. Testing including representative and standardized phantoms (hand, head, torso, etc.) are needed to understand the final device performance. New measurement post processing features allow users to examine results and better understand the radiation properties of the device in these scenarios, enabling research and development engineers to develop better products.

Historically, CATRs have been the preferred solution for testing high gain antennas such as base stations. The features of MVG systems are the high performance feeds, which are designed specifically to maintain high plane wave purity of the quiet zone over very wide bandwidths. Another feature of the MVG systems is the positioner, designed for minimum interference with the device, making it usable also for testing of smaller handheld devices.

The plane wave synthesizer (PWS) array or plane wave generator (PWG) array is an array of elements with suitably optimized complex coefficients, generating a plane wave in close proximity to the array. The PWG can achieve far-field testing conditions in a quiet zone locat-

▲ **Fig. 9 MVG's multi-probe system testing a drone.**

▲ **Fig. 10 MVG's SG3000F automotive test system.**

Fig. 11 NSI-MI's SNF-FIX-1.0 SNF System.

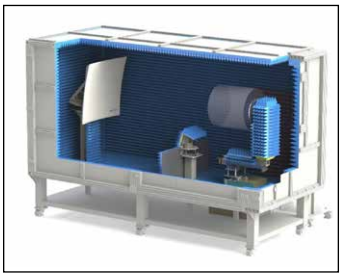

Fig. 12 CAD drawing of NSI-MI's portable CATR system with 80 cm quiet zone.

Fig. 13 R&S ATS800R compact test chamber.

ed in a region close to the array, similar to what is achieved in a CATR but at shorter distance making the system more compact and easier to use. The main features of the PWG systems from MVG are the ability to cover the entire bandwidth for 5G testing in a single system. MVG offers large systems that can accommodate entire base stations, even vehicles (see ***Figure 10***).

National Instruments Solutions

Whenever engineers discuss OTA test solutions, RF chambers almost automatically appear as necessary components of the solution. For design characterization, validation, compliance and conformance tests, a proper RF chamber (anechoic, CATR or reverberation types) provides a quiet RF environment that ensures the design meets all performance and regulatory requirements with sufficient margin and repeatability. However, for volume production, traditional RF chambers can take much of the production floor space, disrupt material handling flows and multiply capital expenses.

To tackle these problems, OTA-capable IC sockets—small RF enclosures with an integrated antenna—are becoming commercially available, enabling semiconductor OTA test functionality in a reduced form factor. Although the measurement antenna is a couple of centimeters away from the DUT IC, that is enough distance for far-field measurements for each individual antenna element. The relatively small size of the socket also facilitates multi-site, parallel tests to multiply test throughput, while minimizing signal power losses. On the other hand, the small socket prevents making beamformed measurements for the whole antenna array, which typically has a far-field distance of 10 cm or longer.

At 28 GHz, a 10 cm distance translates to over 20 dB of free space path loss, as opposed to just 1 dB on an equal length coax cable. Considering a receiver IP3 measurement, OTA methods would require the test instrument to produce 20 dB higher output power at the transmit antenna in order to achieve the same level of received power at the DUT. This can be a challenge for RF chamber-based OTA configurations; however, for OTA socket-based solutions, at 1.5 cm away, it only requires 5 dB higher transmitted power.

With the inclusion of active beamformer electronics, newer generation of 5G active antenna array devices now have many nonlinear RF components, such as digitally controlled PAs, LNAs, phase shifters and mixers. New designs incorporate multi-channel configurations in a single package. NI's software-designed test platform keeps pace with the latest 5G NR PHY layer requirements and includes the measurement science and instantaneous bandwidth necessary to test wide NR component carriers or carrier-aggregated signals. NI's high bandwidth instrumentation also allows for linearization of the DUTs using digital predistortion techniques. The NI platform provides for phase-coherent and time-aligned expansion into multi-channel measurement systems for comprehensive test coverage of the latest NR semiconductor devices.

NSI-MI Solutions

NSI-MI Technologies products for 5G testing include near-field and CATR systems. For near-field testing, NSI-MI recommends pattern testing only with CW tones when possible. The SNF-FIX-1.0 is a spherical near-field system that rotates a probe to any position on a sphere up to $\theta \leq 150°$ around a stationary DUT. It does this with a dual rotary stage articulating arm. The advantage of this system is its ability to sample near-field patterns without the need for any type of rotation of the DUT. ***Figure 11*** shows the SNF test system. If DUT stationarity is not required, the SNF-RAZ-0.7 roll-over-azimuth system may also be used for SNF pattern testing.

For more general 5G testing, NSI-MI recommends a CATR. The chambers designed by NSI-MI can handle mmWave frequencies up to 110 GHz. The CATRs designed for 5G testing are intended for mmWave testing, as those frequencies are the primary driver for OTA testing in 5G. But they can be modified for FR1 OTA testing. They are designed for 30, 50, 80 and 100 cm quiet zones (see ***Figure 12***).

Rohde & Schwarz Solutions

It is difficult to heat up or cool down an entire OTA chamber, more so since the absorber material used in these chambers cannot withstand very high or low temperatures. Neither can the motors in high accuracy positioners. The solution is the use of a relatively small enclosure around the DUT inside the chamber, changing the temperature only inside this enclosure rather than in the entire chamber. Of course, the enclosure itself must have only minimal influence on the radiation parameters or the beam emitted by the DUT.

A typical CATR setup is mounted inside a shielded chamber for RF conformance testing, typically together

with a positioner. However, a chamber takes up space in a space limited R&D environment. R&S created a product where a CATR setup can be put on an engineer's work bench or even inside a 19 in. rack taking up minimal floor space inside the lab, while providing a big and accurate quiet zone for RF and protocol R&D and regression testing (see ***Figure 13***).

For testing antenna array systems, typically a chamber with 3D positioner is required to measure the 3D radiation pattern of the array under test. R&S offers the ATS1000 with a high precision conical cut positioner to fulfill these tasks in a very compact size (see ***Figure 14***). As an additional option, the ATS1000 can be equipped with a "temperature bubble" in which extreme temperature conditions between −40°C and +85°C can be achieved using an external thermal stream. The bubble creates a relatively small closed environment around the DUT so the temperature changes can be achieved quickly. Since the bubble is made out of RF transparent material, the influence on the overall test results can be neglected.

Boonton, Noisecom Solution

The equipment and testing techniques used for engineering and quality assurance will be expensive and time consuming compared to what will be needed on the production line for 5G. Boonton, Noisecom has an interesting approach for OTA testing using a Noisecom calibrated noise source outside the chamber, connected to a transmit antenna inside the chamber. Receive antennas inside the chamber are connected to test equipment outside the chamber. The noise source can have one or two known excess noise ratio (ENR) values with calibration data for the bandwidth of interest. The benefit of having two ENR levels is the ability to determine Y factor noise figure of the DUT for radiated measurements.

An advantage of the noise source is the calibration points can normalize the equipment for power and frequency response. Once the equipment is normalized, the noise source is used to determine and verify the path loss of the interconnects in the system. Since the noise source is generating wide bandwidth OFDM-like signals, with crest factors (CF) similar to those to and from the DUT, it is straightforward to verify the system response to see if anything has changed between tests, perhaps caused by connector wear or operator error.

Fig. 14 R&S ATS1000 test chamber.

Boonton RTP5000 RF broadband RF power sensors can be connected to multiple receive antennas inside the chamber around the DUT (see ***Figure 15***). The RF peak power sensors are capable of measuring the average and peak power being transmitted from the DUT. RF sensors can be synchronized to obtain composite average and peak power and determine CF. CF measurements are a quick figure of merit in a production test environment.

Noisecom noise sources are proven OFDM-like signal generators at a fraction of the cost of expensive signal generators and can be used for verification, calibration and signal source to speed up production tests. Boonton RTP5000 series RF peak power sensors offer a simple and fast way to measure complex OFDM signals using CF as a figure of merit to develop go, no-go testing.

SUMMARY

5G OTA testing will evolve quickly in 2019, as standards are defined and 5G products go into production. There will certainly be several methods needed to test and verify 5G components and systems, as noted in this article. The primary tradeoffs for cost, accuracy and throughput will need to be determined quickly and the test methods standardized as 5G deployments accelerate.■

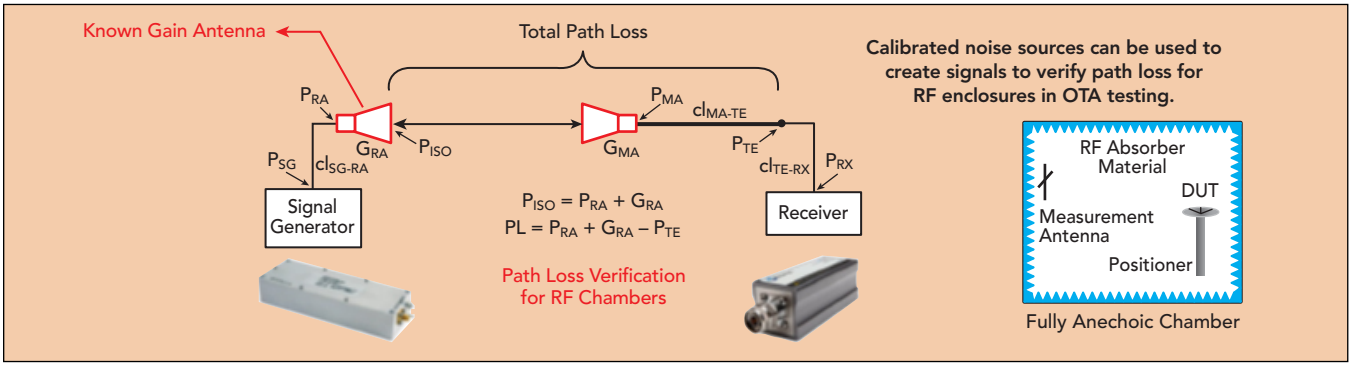

Fig. 15 Boonton, Noisecom's OTA path loss measurement using noise.

Automotive Radar and Congested Spectrum: Potential Urban Electronic Battlefield

Sefa Tanis
Analog Devices Inc., Norwood, Mass.

As automotive radars become widespread, the heavily occupied RF spectrum in an urban environment will resemble an electronic battlefield. Radar will face a combination of unintentional—even intentional—jamming, and designers must implement counter-jamming techniques like ones used in electronic warfare (EW). An automotive radar can experience either denial or deceptive jamming. Denial jamming blinds the victim's radar, reducing the signal-to-noise ratio (SNR) and, as a result, the probability of target detection is degraded. Deceptive jamming makes the victim's radar "see" targets that are really false. The victim's radar loses the ability to track the real targets, and vehicle safety is compromised. These jamming attacks could originate from mutual interference between automotive radars or be deliberate, by simply pointing a strong continuous wave (CW) signal into the victim's radar using inexpensive hardware.

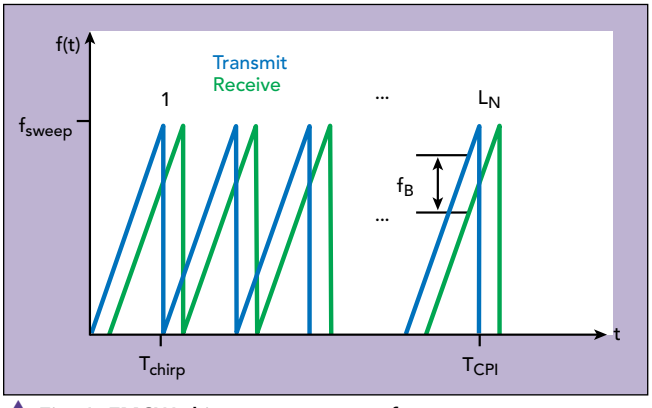

Fig. 1 FMCW chirp sequence waveform.

While current jamming avoidance techniques may be adequate today, with the proliferation of radar sensors, more resilient mitigation techniques will be needed, either stand-alone or in conjunction with other approaches. Such techniques include time/frequency domain signal processing or complex radar waveforms.

JAMMING FMCW RADAR

The waveform is a critical system parameter that determines the radar's performance in the presence of jammers. Automotive radars in the 77 GHz band mainly use FMCW waveforms, where a CW signal is linearly swept or "chirped" in frequency across the RF band (see ***Figure 1***). The frequency difference or beat frequency (f_B) between the transmit and receive signals is proportional to the distance to the target (R) and can be determined by

$$f_B = \frac{2}{C}\frac{f_{sweep}}{T_{chirp}}R \ ,$$

where f_{sweep} is the change in frequency and T_{chirp} is the time for the frequency sweep.

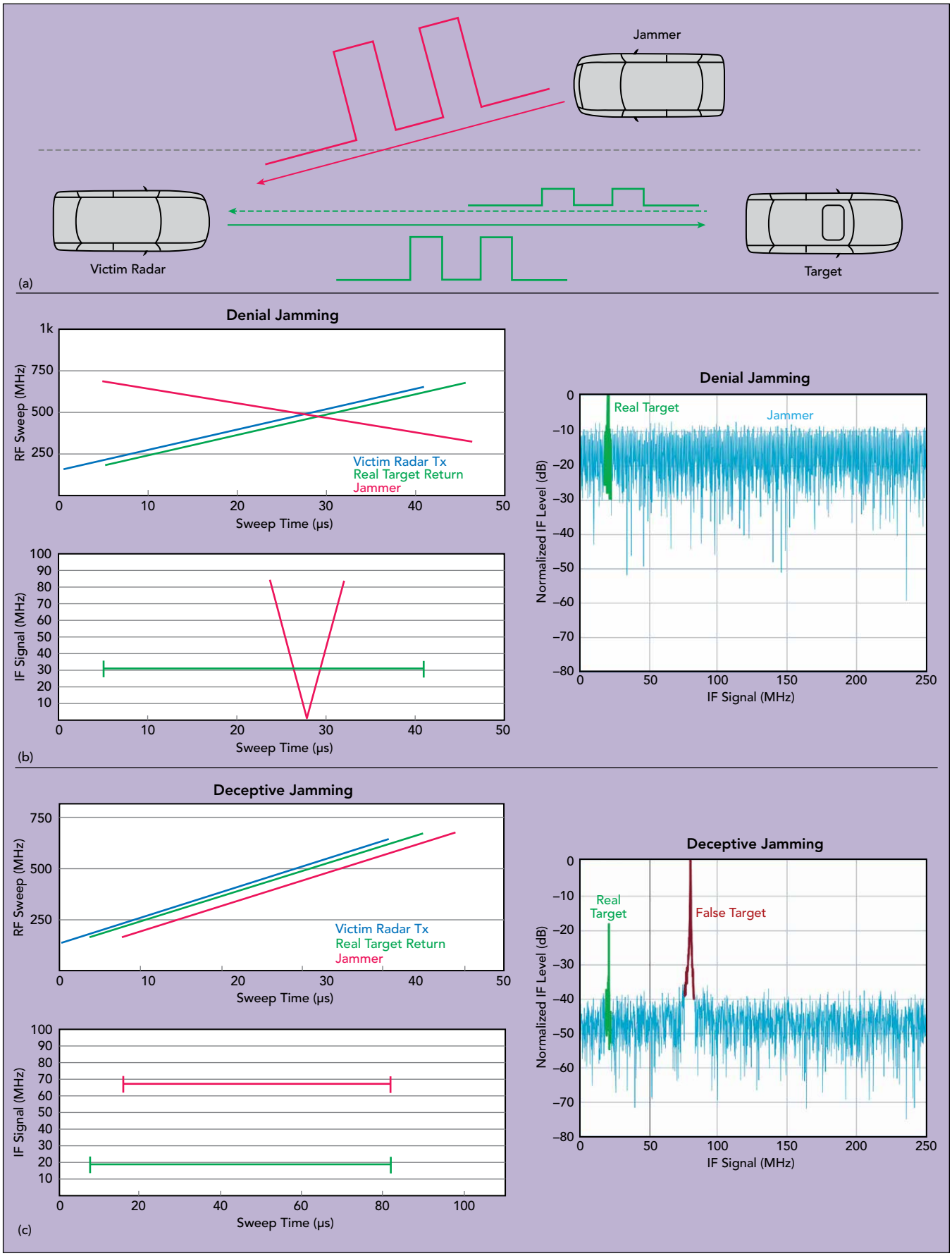

▲ **Fig. 2 Driving scenario (a) with denial jamming (b) and deceptive jamming (c) of an FMCW radar.**

Unintended jamming can occur in a dense RF environment when FMCW radar sensors are operating in the same portion of the frequency band. A typical automive jamming example is shown in ***Figure 2a***.

Denial Jamming

An arbitrary FMCW jamming signal that falls in the receiver bandwidth of the victim's radar raises the noise floor (see ***Figure 2b***). Called denial, this jamming may cause small targets—those with small radar cross section (RCS)—to disappear, due to the poor SNR. A denial attack could be purposeful, by simply beaming a strong CW signal into the victim's FMCW radar.

Deceptive Jamming

If the swept frequency of the jamming signal is delayed and synchronized with the victim's radar, the impact is a false target generated at a fixed range (see ***Figure 2c***). This technique is commonly used by EW jammers. However, this can occur unintentionally with an oncoming automobile having a similar FMCW radar, although the probability of time alignment between the victim and jamming radars is small. Nonetheless, a jammer delay offset less than the maximum range delay of the victim's radar could look like a real target. For example, a radar with 200 m maximum range would require sweep alignment of less than 1.3 µs. Such a deceptive attack could be intentional using sophisticated EW equipment mounted on the oncoming automobile.

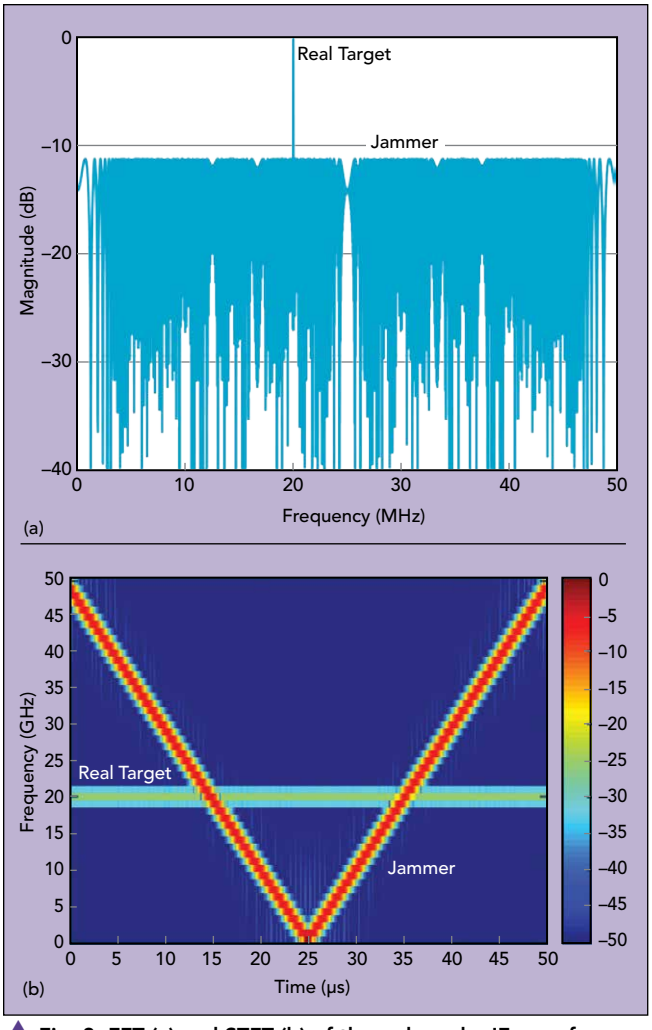

▲ **Fig. 3 FFT (a) and STFT (b) of the radar echo IF waveform with jamming.**

Generally, deceptive jamming is based on retransmitting the victim radar's signal with a systematic change in delay and frequency. This signal can be noncoherent, in which case the jammer is called a transponder, or coherent, termed a repeater. Repeaters receive, alter and retransmit one or more jamming signals, while transponders transmit a predetermined signal when the desired victim's signal is detected by the jammer. A sophisticated repeater-based attack typically requires a digital RF memory (DRFM). A DRFM is capable of carrying out coordinated range delay and Doppler gate pull-off attacks, with the false target range and Doppler properties maintained to deceive the victim's radar.

JAMMING MITIGATION

Basic radar jamming mitigation techniques rely on avoidance. The objective is to reduce the probability of overlap in space, time and frequency, using methods such as:

- Spatial: Using a narrow and electronically-scanned beam to reduce the risk of jamming. A typical field of view for long-range automotive cruise control radar is ±8 degrees. Nonetheless, a strong jammer could be effective via the antenna sidelobes.
- Temporal: Randomizing the FMCW chirp slope parameters to avoid periodic jamming.
- Spectral: Randomizing the FMCW chirp start and stop frequencies to reduce the probability of overlap and jamming.

The basic methods of randomization would avoid accidental synchronization with other radars but might not be as effective in dense RF environments. The growing number of radar sensors will require more sophisticated techniques to mitigate possible jamming.

Detect and Repair

An alternative method to avoid jamming is to repair the received waveform using signal processing algorithms. Time/frequency domain techniques can be effective against denial type jamming. In the oncoming automobile scenario (see Figure 2), the jammer sweeps all frequency bins for a very short time duration. This fast time-varying signal manifests itself as a raised noise floor in the fast Fourier transform (FFT) domain. Time/frequency domain signal processing transfers the signal to another domain where it is easier to filter out the jamming.

For time-varying signals, a short time Fourier transform (STFT) provides more information than a regular FFT, and STFT-based techniques can be used for countering narrowband jamming (see ***Figure 3***). The STFT essentially moves a window through the signal and takes the FFT of the windowed region. The signal is filtered in the frequency domain to remove the jammer components before being transformed back to the time domain. ***Figure 4*** shows a typical FMCW jamming scenario of overlapping RF chirp sequences and the IF signals obtained using STFT processing. The plots on the right show the beat signal from mixing the radar (blue) and jamming (orange) signals. A horizontal line indicates

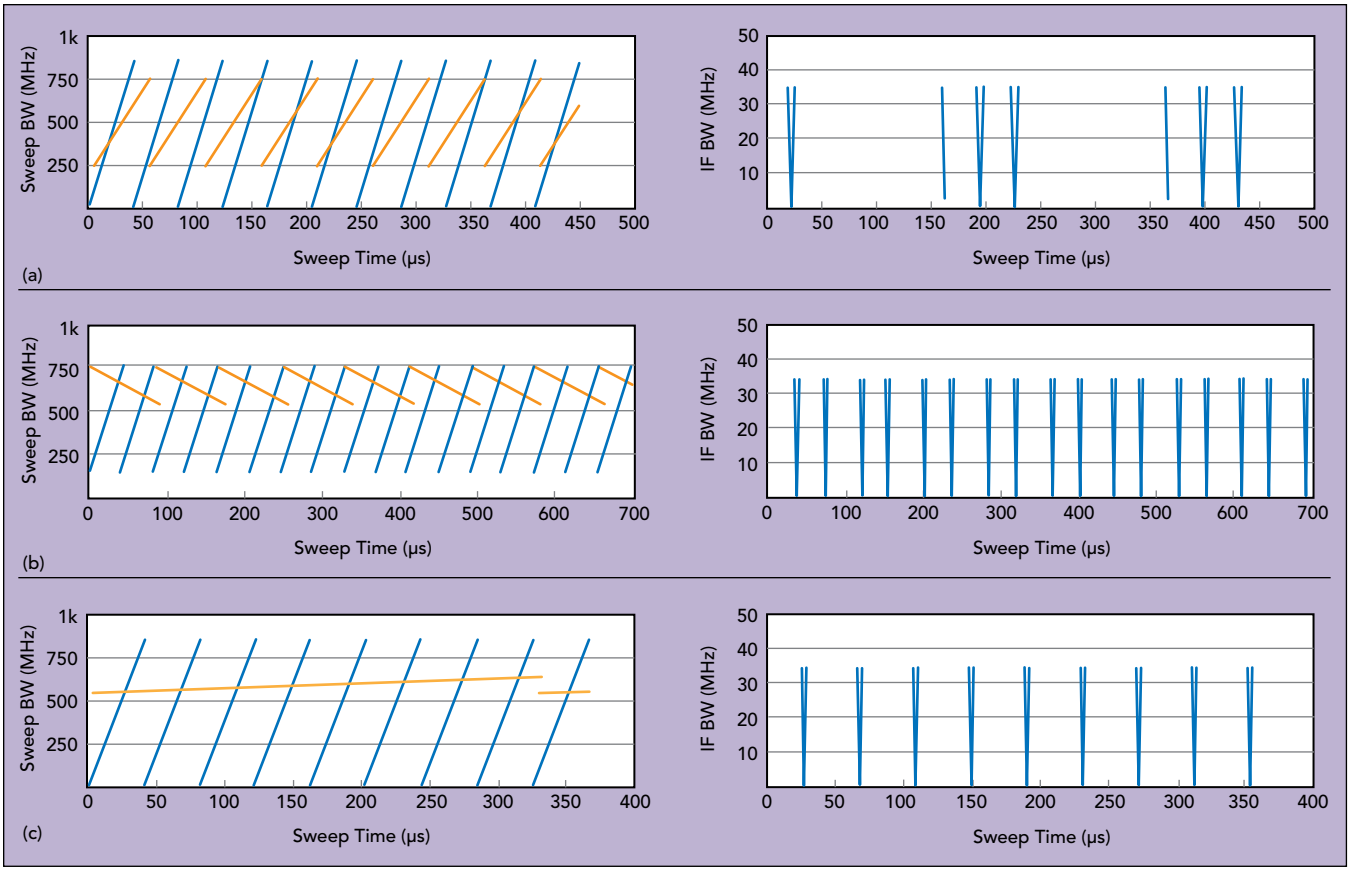

▲ **Fig. 4 Radar and jammer chirps (left) and STFT-processed IF (right) for similar direction (a), opposite direction (b) and CW interference (c) scenarios.**

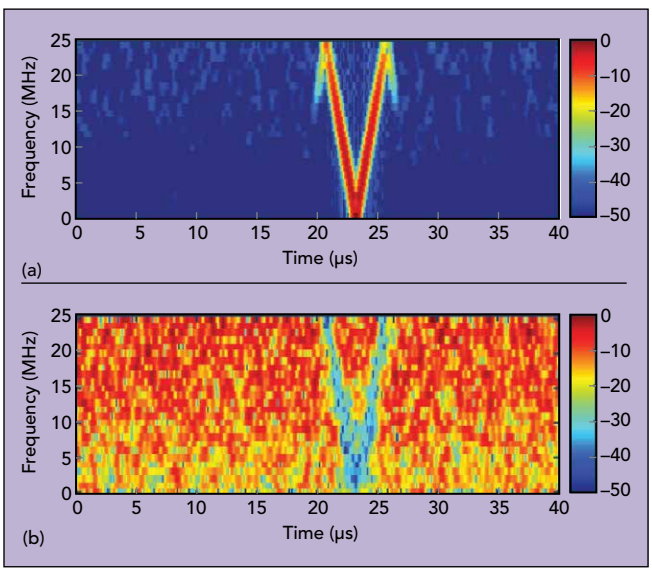

▲ **Fig. 5 STFT chirp return with strong interference (a) and after amplitude-based masking (b).**

a target, while V-shaped vertical lines indicate the presence of a jamming signal. Similar or opposite direction FMCW jamming or a CW-like slow chirp have similar effects on the IF signal. In all these jamming scenarios, the fast moving V-shaped IF signal raises the noise floor in the regular FFT domain, as was seen in Figure 3.

Amplitude-based masking can be used to filter out jamming in the STFT domain. This assumes, of course, that the victim's radar front-end and quantization have enough dynamic range to linearly process the stronger jammer signal and the small intended target at the same time. ***Figure 5a*** shows the STFT signal with a strong jammer, and ***Figure 5b*** shows the STFT after amplitude-based masking. Without processing, multiple real targets will not be visible in the presence of a strong jammer; however, amplitude-based masking excises the V-shaped jammer in Figure 5b, enabling the low SNR targets to be discerned when transformed back to the time domain.

While STFT-based jamming mitigation can be used against strong jammers in denial jamming scenarios, with deceptive jamming attacks, STFT alone cannot authenticate whether the return signal is real or false.

Encrypted RF

The simple countermeasure to reduce the impact of deceptive jamming from repeater attacks is using a low probability of intercept (LPI) radar waveform. The objective of an LPI radar is to escape detection by spreading the radiated energy over a wide frequency spectrum, usually via a quasi-random sweep, modulation or hopping sequence. FMCW is a type of LPI waveform, and if phase coding or encryption is used with the frequency chirp, it is possible to further reduce the probability of a DRFM intercepting the radar signal. An encrypted RF

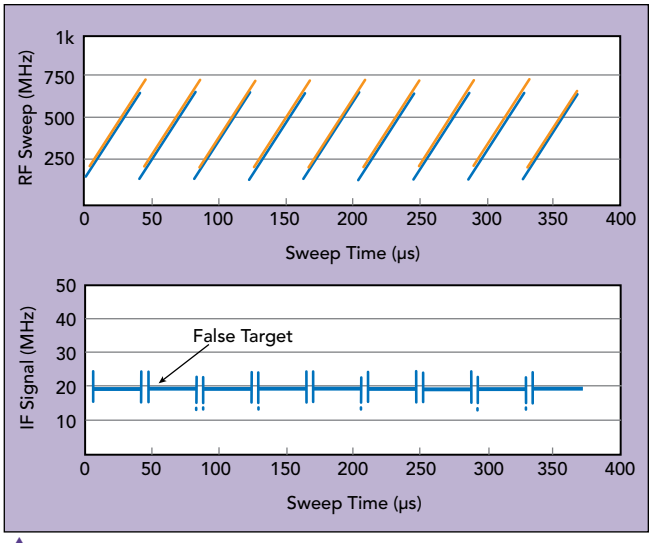

Fig. 6 Jamming due to identical radars with frequency offset and delay.

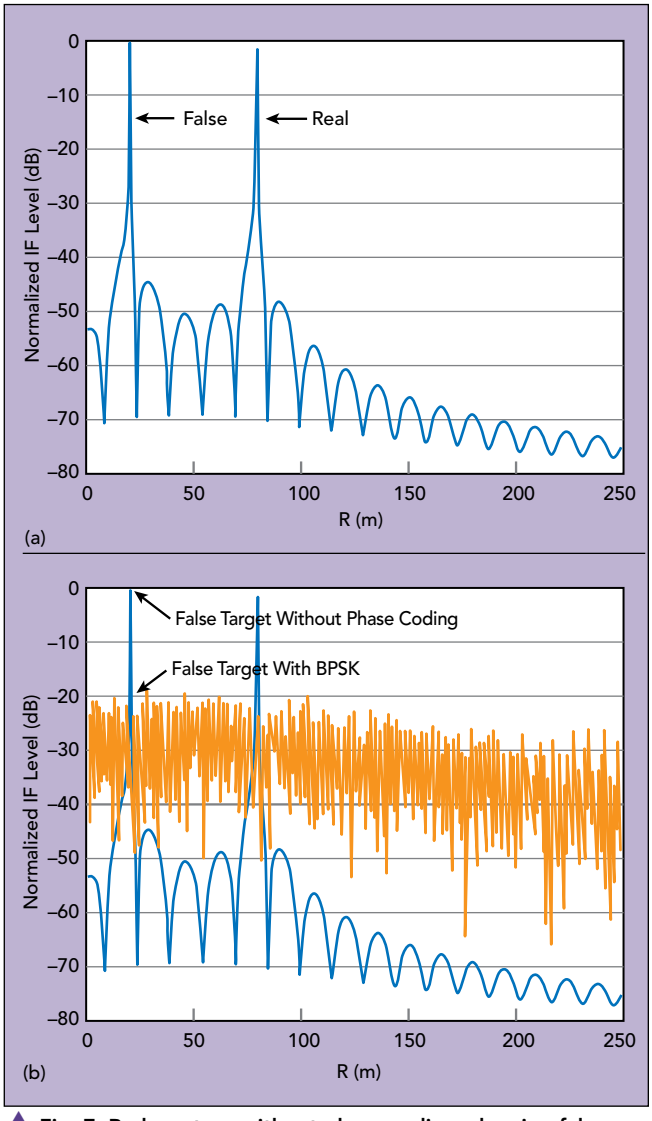

Fig. 7 Radar return without phase coding, showing false and real targets (a). Phase coding reduces the false target by some 20 dB (b).

signature unique to each radar sensor can authenticate the return signal.

Figure 6 shows a use case where two identical radars are on two different automobiles, and the frequency offset and delay between them generates a false target in the victim's radar. The jamming radar is time aligned with the victim radar, i.e., having the same chirp slope and a short offset. Phase-coded FMCW radars will provide high jamming robustness in this case, and the use of orthogonal codes will also make MIMO radar operation possible, by enabling multiple simultaneous transmit waveforms.

The requirements for coding are:

- Code length: The code length should achieve minimal range sidelobe levels with short sequences. A pseudo-random-noise (PRN) sequence length of 1024 results in a peak sidelobe level (PSLL) of about 30 dB, i.e., $10 \bullet \log_{10}(1024)$. Transmit codes together with receive filter weights can be optimized to improve the PSLL at the expense of SNR.
- Good cross-correlation properties: Cross-correlation coefficients of the members of a set should be zero to achieve separation between sensors.
- Doppler resistance: Phase-coded radar performance can suffer from the Doppler shift. Binary codes are Doppler intolerant, while polyphase codes degrade less rapidly.
- Available number of different codes: A large family size is better to assign a unique code to each radar sensor.

Figure 7a illustrates a radar echo with no phase coding, where the jamming signal appears as a false target. When the transmitted FMCW waveform is phase-coded with a PRN sequence, the jamming signal is suppressed, as shown in ***Figure 7b***. The dynamic range is compromised with this method; however, the radar signal processor could use phase-coded FMCW for a few chirps to flag a false target, then switch back to normal operation.

FUTURE TRENDS

In congested automobile radar environments, jamming can be mitigated using advanced signal processing algorithms and complex waveform generation techniques. STFT-based signal processing can be used against denial attacks. Phase-coded FMCW provides an additional layer of resistance to both noncoherent and coherent deceptive attacks by using processing gain and interception avoidance. ***Table 1*** summarizes these mitigation techniques. The jamming mitigation principles for automotive radar are also applicable for other radar sensors: robotics, road tolling, GPS and UAV landing or collision avoidance systems.

Currently, automotive radar sensors are operating in a non-cooperative mode, i.e., not communicating with each other. Although a cooperative mode of operation requires industry-wide harmonization, the arbitration between radar sensors would help resolve interference. A future radar concept including sensor cooperation is the fusion of communication nodes and radar sensors. Future radars with complex waveforms offer the possibility to include information in the radar signal, enabling the

same hardware to be used simultaneously for radar and communications (RADCOM). Such a capability has the following benefits:

- Multi-user capability without interference.
- Coding the radar signal with OFDM or similar communication codes enables information to be contained in the radar signal.
- Simultaneous RADCOM.

5G mmWave transceivers with multi-GHz bandwidth and beam steering capabilities are candidates for use in a RADCOM system.■

TABLE 1

JAMMING MITIGATION FOR FMCW AUTOMOTIVE RADAR

Jamming Type	*Denial*	*Deceptive*	
Jamming Hardware	Another Radar Sensor or a Simple CW Generator	DRFM (Coherent)	Transponder (Noncoherent)
Impact on Victim Radar	Poor SNR	False Target	
Resilient Mitigation Technique	STFT	Phase-Coded FMCW	
Mitigation Principle	Repair the Radar Return Waveform	Escape Detection	Processing Gain of the Coding Sequence
Mitigation Effectiveness	High	Moderate	Good

Steering Circuit Materials for 77 GHz Automotive Radar

John Coonrod
Rogers Corporation

Advances in semiconductors are pushing practical frequencies well into the millimeter-wave (mmWave) range and enabling such applications as affordable automotive radar systems at 77 GHz. These radar safety systems will inevitably also become integral parts of the "self-driving," autonomous vehicles of the future, driven by high volume, commercial mmWave devices and components. Of course, not to be forgotten, is the importance of the high frequency circuit materials used for the printed circuit boards (PCBs) in those 77 GHz automotive radar applications. Many new circuit materials are being formulated for these higher frequencies although they may not all be best suited for such high frequency use. Just what circuit material properties are most critical at mmWave frequencies? A review of those properties may help to simplify the selection of optimum circuit materials for mmWave applications, especially for 77 GHz automotive radar systems.

The higher frequencies represent valuable commodities: available bandwidths. As cell phones, WLANs, and other commercial applications have gobbled up lower frequency bands, mmWave frequencies such as 60, 77, and even 94 GHz are providing bandwidths for such emerging applications as Fifth Generation (5G) cellular systems and automotive radar. Understanding how essential material properties should fare at mmWave frequencies is an important starting point in specifying circuit materials not just for 77 GHz but for a growing list of high frequency applications above about 28 GHz.

CRITICAL PROPERTIES

Six critical circuit material properties for 77 GHz radar (and other mmWave) circuit designs are dielectric constant (Dk), relative permittivity (ε_r), dissipation factor (Df), loss tangent or tan delta, copper surface roughness, thermal coefficient of Dk (TCDk), moisture absorption, and glass weave effect. It is rare for a high frequency circuit material to excel in all six properties at mmWave frequencies. In addition, given the fine circuit dimensions at the small wavelengths of mmWave frequencies, PCB fabrication options can play a hand in a choice of circuit material for such high frequency circuits. It can be very difficult to find a circuit material that provides high grades in all six material properties and which also lends itself to repeatable and reliable circuit fabrication.

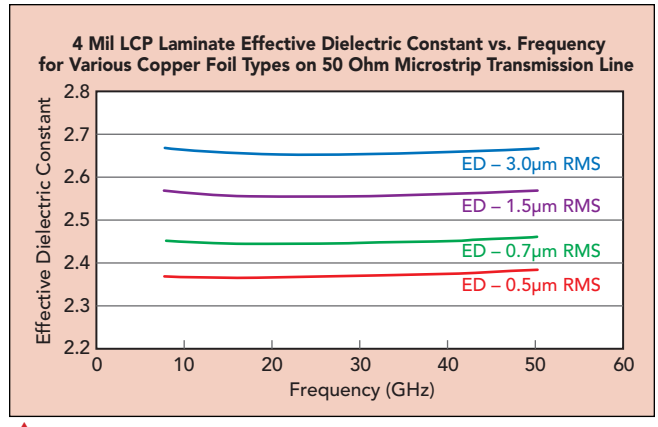

Fig. 1 Effective Dk vs. frequency, using 50-Ω microstrip transmission-line circuits and showing differences due to copper surface roughness only.

DIELECTRIC CONSTANT

Any consideration of circuit material Dk for 77 GHz automotive radar and other mmWave circuit applications really has two sides to it: for the raw substrate it-

self and related to how the Dk will impact the circuit, also known as Design Dk. For the raw substrate, the Dk can be considered in terms of its tolerance and the Dk dispersion. Dk tolerance is a material parameter that is determined by the manufacturing variables involved in making the laminate, and tighter tolerances may be required for some applications. Based on experience with higher frequency, mmWave circuits, a Dk tolerance of ±0.050 is usually acceptable. Dk dispersion, which is a natural property of material, refers to changes in Dk with frequency. It is typically more important for wideband applications, where a material must handle signals across many different frequencies, rather than in narrowband applications, such as 77 GHz, where only a narrow range of frequencies is being handled.

Design Dk is a form of "working value" of Dk determined from measurements of a material in circuit form. Design Dk[1-3] is affected by many variables, making it difficult to assess variations in the parameter. It is well established that electromagnetic (EM) waves through a circuit medium will be slowed by any increase in the material's Dk. But other factors, such as the copper roughness of the circuit material which impacts the phase velocity of the EM wave, can affect the performance of a circuit material at 77 GHz and other mmWave frequencies ***(see Figure 1).***[2]

As shown in Figure 1, four different laminates and circuits were formed, all based on the same substrate material, 4-mil-thick LCP. This is an isotropic substrate which is well behaved across a wide range of microwave and mmWave frequencies. The four laminates differ by copper surface roughness, with four different copper types used. The surface roughness of the different copper metals, which is the copper surface at the substrate-copper interface, was measured prior to forming the copper-clad laminates. The laminates were then sent to a PCB fabricator to make 50 Ω microstrip transmission lines on each laminate. For each data set, two circuits identical in every way except physical length were evaluated. By having one circuit much shorter than the other, the microstrip differential phase length method was used to obtain the effective Dk versus frequency. As Figure 1 shows, the circuits with the smoothest copper have the lowest effective Dk. Circuits with laminate of rougher copper show a trend of increased effective Dk. The difference in effective Dk among the circuits is about 0.3, with the only difference in the circuits being the copper surface roughness.

For Design Dk, circuits using thinner materials are more impacted by conductor effects than circuits using thicker materials. For example, if the Figure 1 study was performed with a thicker substrate, the differences in the effective Dk values for the different copper surface roughness would be much less. As the slight curvature of the four effective Dk plots would indicate, there is some normal dependency on frequency. Some of the changes in the curves are related to the dispersive nature of microstrip transmission lines and some are a result of the material dispersion. When the Dk is extracted from the effective Dk data, the Dk versus frequency curve, which is the Design Dk curve for the material, will typically have a slight negative slope as shown in Figures 2a and 2b.

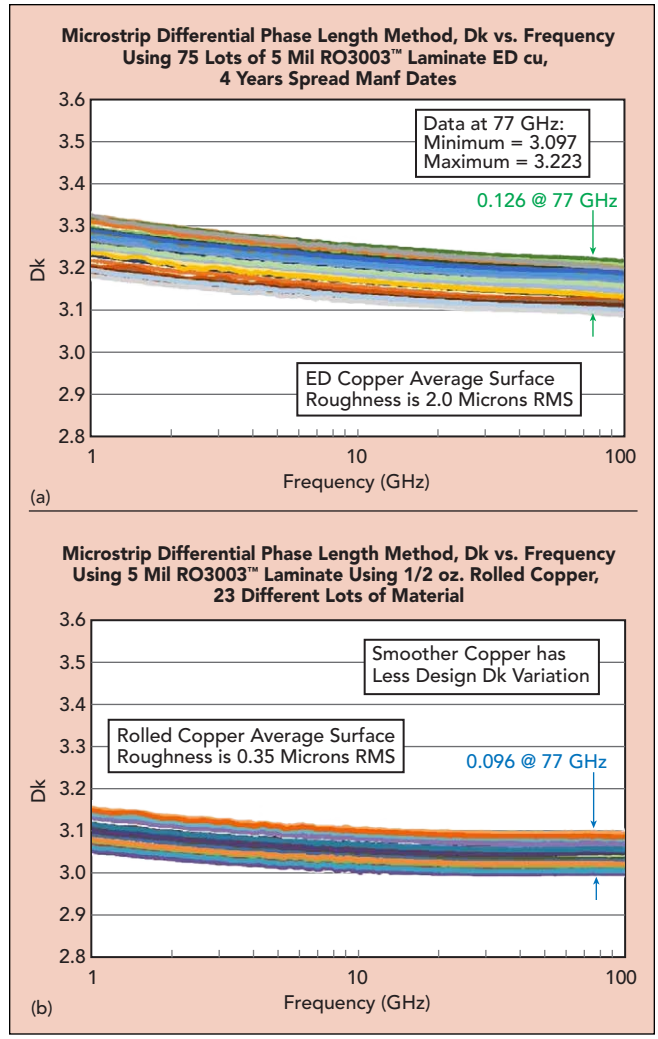

Fig. 2 Microstrip transmission-line testing use multiple lots of 5-mil-thick RO3003™ circuit material with ED copper (a) and rolled copper (b).

The Dk versus frequency curves shown in ***Figures 2a*** and ***2b*** show correct trends, with a slight negative slope with increasing frequency. When the microstrip dispersion is removed in the Dk extraction process, the remaining material dispersion will cause the slight decrease in Dk with frequency. The range of Design Dk values (around 3.1) may appear large, but it is not since many variables can affect Design Dk. For this particular material, the raw material Dk varies by only ±0.040 or a range of 0.080. Some variations will also occur due to circuit fabrication, such as variations in conductor width and variations from trapezoidal effects. Trapezoidal effects refer to the shape of the signal conductors, which might appear ideally in a rectangular cross-sectional shape but appear more trapezoidal in shape. Variations in the conductor shape result in variations in current density and in fringing fields and at higher, mmWave frequencies, these effects can impact performance. Variations in the curves shown in Figure 2 are also related to the tolerance of the substrate thickness, variations in final copper plating thickness, and variations in the copper surface roughness.

COPPER ROUGHNESS

Electrodeposited (ED) copper, such as used on the circuits shown in Figure 2a, will exhibit normal surface roughness variations; the average surface roughness for the ED copper used with these circuits is 2.0 µm RMS, although this copper surface roughness can vary from 1.8 to 2.2 µm. For circuits on the smoother side of this roughness variation range, the Design Dk will be lower in value, while for circuits fabricated with rougher copper, the Design Dk will be higher in value. For the Design Dk range in Figure 2a (0.126 at 77 GHz), considering the many variables that can affect it, this is a well-controlled Design Dk tolerance of ±0.063.

Compared to Figure 2a, Figure 2b shows much less variation in Design Dk for the same circuit substrate using smoother, rolled copper instead of ED copper. This shows that very smooth copper can provide less variations in Design Dk, although the curves can also be somewhat misleading since PCB fabrication techniques can be different for substrates with rolled copper compared to substrates with ED copper.

Copper surface roughness and its variation also impacts the insertion loss of high frequency microstrip circuits. Rougher copper surfaces cause higher conductor loss and ultimately more insertion loss. Insertion loss is also dependent upon the circuit substrate thickness, where thinner circuits are more impacted by the copper surface roughness than thicker circuits. For example, for circuits fabricated on the same substrate and comparing different thicknesses of substrate with different copper surface roughness, the insertion loss difference between a thin circuit using smooth and rough copper is more significant than the insertion loss difference between a thick circuit using copper that is rough and smooth. In the case of a circuit using 5 mil thick RO3003 materials, the insertion loss difference at 25 GHz for a circuit using rough ED copper compared to a circuit using smooth rolled copper is 0.35 dB/in. For a similar comparison using 20 mil thick RO3003 laminate with rough ED copper and smooth rolled copper shows an insertion loss difference of 0.10 dB/in. This shows that the thinner circuit is more impacted by copper surface roughness differences than a thick circuit, and most mmWave circuits are fabricated on relatively thin materials.

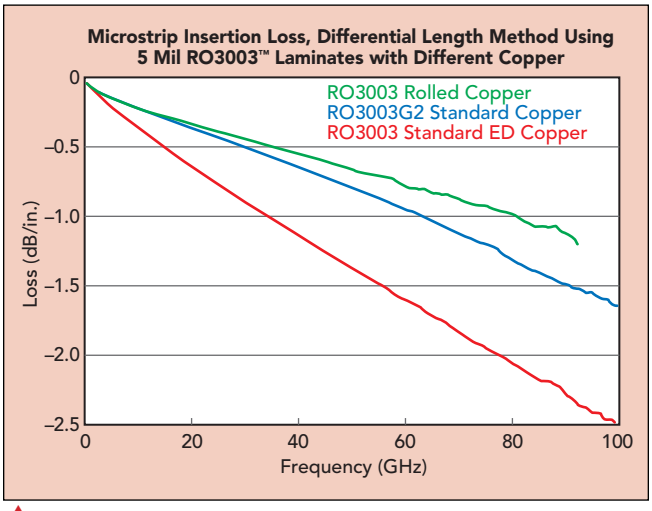

Fig. 3 Microstrip insertion loss curves are for circuits based on 5-mil-thick substrates with similar Dk values but with copper having different surface roughness, commonly used in 77 GHz applications.

To show the effects of copper surface roughness, ***Figure 3*** presents microstrip circuits on two similar circuit materials with the same (5 mil) thickness but with different copper surface roughness. These are materials currently used in 77 GHz applications. The RO3003 material has been available for some time; the RO3003G2™ material, also from Rogers Corp., is relatively new and based on RO3003 laminate but optimized for 77 GHz automotive radar applications. The differences shown in insertion loss are due mainly to copper surface roughness, since the two materials have similar Dk and Df values. The average copper surface roughness for the RO3003 materials using standard ED copper is 2.0 µm RMS, while the same material using rolled copper has a copper surface roughness of 0.35 µm RMS. The RO3003G2 material uses very low profile (VLP) ED copper and features an average surface roughness of just 0.7 µm RMS.

This VLP ED copper of RO3003G2 laminate provides significant improvements in insertion loss compared to the ED copper of RO3003 laminate, but it is not quite as good as rolled copper. But rolled copper is much more expensive than ED copper. The VLP ED copper is slightly more expensive than ED copper, but with cost savings compared to more expensive rolled copper and with obvious improvements in insertion loss performance. Smoother copper, such as VLP ED copper, will also provide more consistent phase angle responses for circuits made with substrates using this copper. For the micro-viaholes commonly used in 77 GHz automotive radar circuits, smoother VLP ED copper is beneficial for laser drilling of the micro-viaholes. Additionally, a laminate which uses small, spherical filler particles is advantageous for the laser drilling process. Through the consistent laser drilling and the use of smaller filler particles, repeatable circuit performance becomes more achievable at mmWave frequencies such as 77 GHz.

THERMAL COEFFICIENT OF DK

Given the wide operating temperature range of automotive sensors, TCDk is an extremely important circuit material property and a measure of how much the material's Dk will change with temperature. For many applications, an acceptable TCDk value should be less than |50| ppm/°C. The value is shown as an absolute value because TCDk can be a positive or negative number. A value closer to zero indicates a Dk with the least amount of change with temperature. As ***Figures 4a*** and ***4b*** show, the Dk can change quite a bit with frequency and temperature. The plots compare two 5 mil thick laminates: RO3003G2 and a competitive material.

MOISTURE ABSORPTION

The operating environment for 77 GHz automotive radar circuits within a vehicle and where it travels is truly hostile and can include the effects of moisture absorption. The circuit material moisture absorption parameter is essentially a measure of the amount of moisture that can be absorbed by a circuit material within a given en-

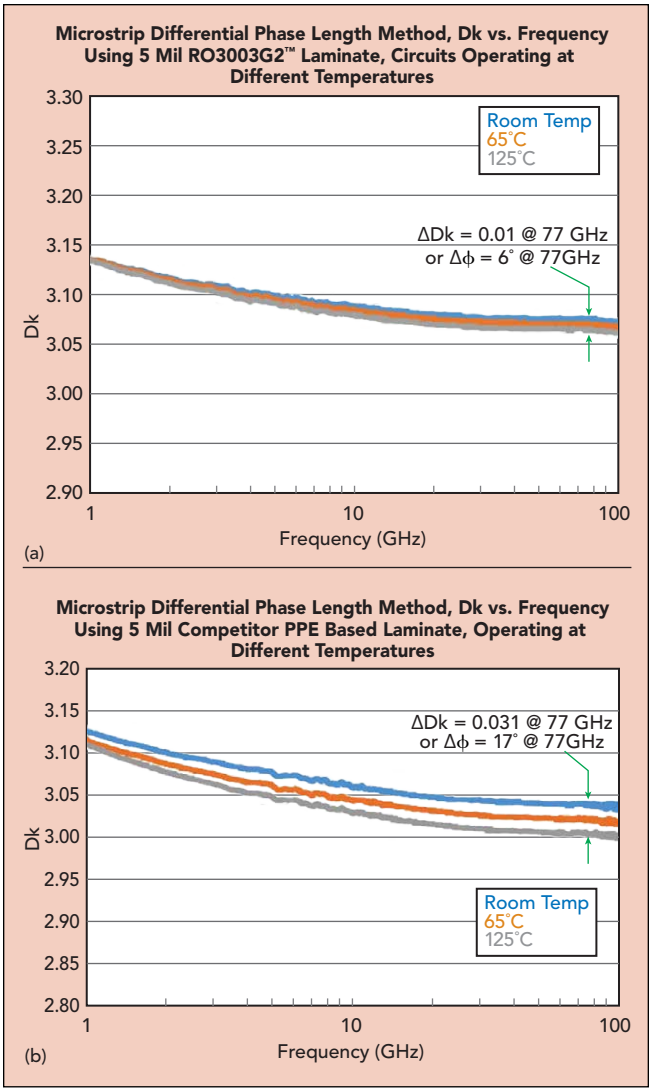

Fig. 4 Microstrip transmission-line testing, with circuits at different temperatures, using material optimized for automotive radar at 77 GHz (a) and a competitive PPE-based laminate (b).

vironment. Water vapor is polar and causes increased PCB insertion loss and will also raise the Dk of the circuit material. Since phase angle consistency is critical for 77 GHz automotive radar applications, any effects of circuit material moisture absorption on phase angle consistency are a concern; phase angle typical increases with an increase in circuit moisture absorption. To evaluate these effects, testing was performed on RO3003G2 circuit material and on a PPE-based high frequency material. Testing compared phase angle differences for circuits at room-temperature conditions (+23°C and 30% RH) and then tested again after being conditioned at +85°C and 85% RH for 72 h. As ***Figure 5*** indicates, moisture absorption can make a difference depending upon material, and reducing the impact of moisture absorption on phase angle can have a significant effect on the performance of a 77 GHz automotive radar system.

WEAVING GLASS

Many high frequency circuit materials depend on glass reinforcement layers for strength; unfortunately, the glass weave effect can impact circuit performance,

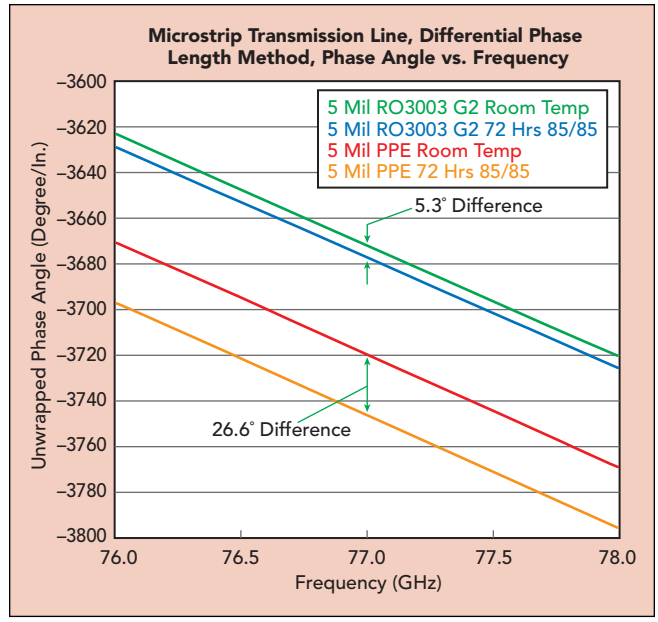

Fig. 5 Microstrip circuits were tested for unwrapped phase angle differences by comparing circuits under room-temperature (RT) conditions and after treatment of 72 h at +85°C and 85% RH.

especially at 77 GHz and at mmWave frequencies. The glass weave pattern used to strengthen a circuit material can also cause differences in Dk throughout the circuit material. Fortunately, some high frequency circuit materials, notably RO3003 and RO3003G2 laminates from Rogers Corp., do not use woven glass reinforcement and the glass weave effect does not apply to them.

Figures 6a, 6b, and ***6c*** provide different views of the glass weave effect. A 1080 glass is used in Figure 6a and, as the picture shows, the formation of glass bundles and glass knuckles, along with open areas having no glass, can result in areas around the circuit material with different Dk values. The Dk of the glass is approximately 6 and the Dk of the resin system will be much less (usually around 2.1 to 2.5) to get a laminate with an overall Dk of about 3 which is used in automotive 77 GHz applications. In general, the contrast between the areas with glass bundles and areas with no glass is not large enough to cause issues at 77 GHz, although some glass styles can have dimensions that equal a fraction of a wavelength at mmWave frequencies and may present issues at 77 GHz.

The opening in the 1080 glass is approximately 10 mils (0.25 mm) and for a microstrip circuit using a laminate with a Dk of about 3, the wavelength is about 97 mils (2.46 mm) at 77 GHz. A fraction of a wavelength can cause resonances and disturbances to propagate signal waves; typically, if the circuit medium has an anomaly that is 1/8th wavelength or less in size it will not cause an issue with a propagating signal wave. A 1/8th wavelength for this type of circuit is about 12 mils (0.31 mm), which is close enough to be a concern.

The glass weave effect may not be seen when only comparing a few circuits against each other. It is probable that glass weave effect may be seen when comparing a large number of circuits against each other. The probability increases as the frequency increases. This is

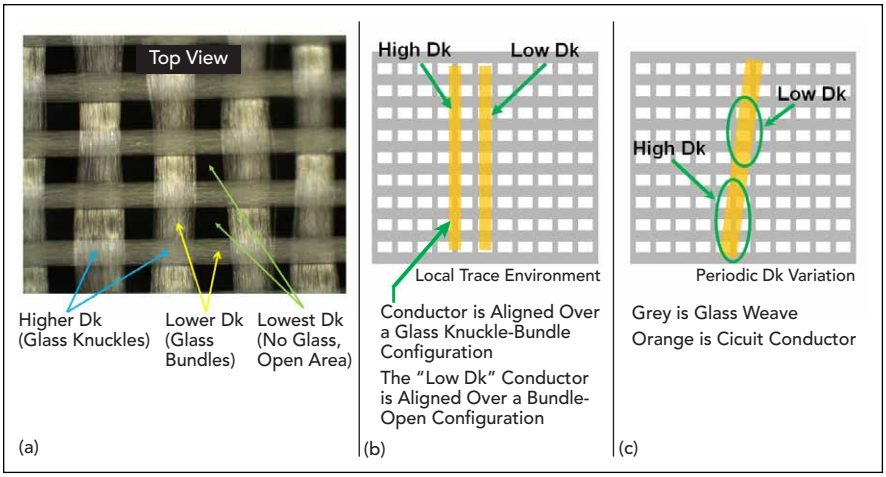

Fig. 6 The glass weave effect in circuit materials can be seen from the picture of a woven glass layer (a), a drawing showing how two circuit conductors can have different Dk values due to the glass weave effect (b), and (c) how the glass weave effect can cause a circuit conductor to have a periodically varying Dk (c).

seen many times in millimeter wave frequency applications such as 77 GHz automotive radar sensors. The main concern for the glass weave effect is shown in Figure 6b, where the circuits align with the glass weave pattern in such a way that one circuit may have a much different Dk medium than another circuit with the same circuit material and with the same circuit design. The periodic Dk resulting from the glass weave pattern in Figure 6c is also a concern. In this pattern, a stepped-impedance structure is formed by regions of high and low Dk due to the angled alignment between the circuit design and the glass weave pattern. If a large number of circuits is evaluated, this slightly angled alignment is much more common than most engineers would assume because the glass weave pattern is not always a perfect grid. There can be large areas of the glass weave that are skewed and even if the circuit pattern is a grid, the glass weave pattern may not be a grid in some areas of the circuit.

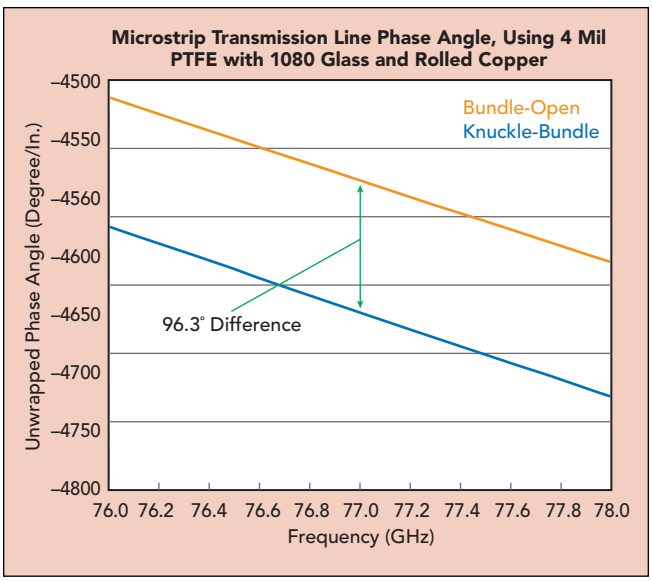

Fig. 7 The plots show differences in phase angle vs. frequency for microstrip circuits of the same design and same material (4-mil-thick PTFE), but aligned according to Figure 6b for high and low Dk.

Studies[4] regarding the glass weave effect were performed in late 2018 and a webinar presented in October of 2018 (and available on the Microwave Journal website). Many configurations were considered, with focus in one study given to knuckle-bundle and bundle-open glass-dielectric patterns (like Figure 6b) because of problems reported due to similar issues with PCBs in 77 GHz automotive radar. In this study, a thin laminate (4 mils or 0.102 mm) based on pure PTFE and rolled copper was used. Four different laminates were analyzed, with the main difference among them being different glass reinforcement layers. The rolled copper helped minimize surface roughness variations. The use of pure PTFE presented a worst case scenario, using a circuit material without a filler. Filler particles can dampen any Dk differences between areas with and without glass.

Hundreds of circuits were fabricated for this study and inspected to find the ideal glass conductor alignment to evaluate differences in circuits having high and low Dk due to a local trace environment like Figure 6b. ***Figure 7*** offers a summary chart for the impact of the glass weave effect on phase response as a function of frequency through 77 GHz.

Figure 7 shows plots of phase versus frequency for microstrip circuits on pure PTFE circuit materials with 1080 glass reinforcement; the glass is an unbalanced open-weave style. Another glass style commonly used for thin circuit laminates is 106 glass. The 106 glass was also included in this study. It is an open-weaved glass, balanced and with small dimensions. The glass styles are termed balanced or unbalanced depending on the amount of glass density on the two axes of the glass. It is balanced when there is approximately the same density of glass on one axis of the glass weave as the other and unbalanced when they are not. The data shown in Figure 7 is for circuits using 1080 glass, however, when testing was performed on circuit materials using 106 glass, the difference in phase angle was 64.7 degrees/in. of microstrip line at 77 GHz.

Circuit material with spread glass was also used in this study. As the name implies, on one axis, the glass bundles are spread, with an appearance like a pane of glass. Glass knuckles still occur, but there are either no open areas or open areas that are extremely small and typically less than 1 mil (0.025 mm). The spread glass used in the study was 1078 glass. Using the same testing applied to the 1080 glass in Figure 7, a phase angle difference of 13.4 degrees/in. of microstrip line was found at 77 GHz.

As is apparent, the glass weave effect can have an impact on the electrical performance of circuit materials, especially for 77 GHz automotive radar and other mmWave applications. When performance is critical

at higher frequencies, circuit materials are available without glass reinforcement: circuit materials such as RO3003 and RO3003G2 laminates from Rogers Corp. are produced without woven glass reinforcement and do not suffer the many effects caused by forming high frequency circuits on substrates with woven glass reinforcement. While woven glass reinforcement may ease some aspects of the PCB fabrication process, homogeneous substrates without woven glass ensure predictable and reliable performance for 77 GHz automotive radar and other microwave and mmWave applications.

References

1. John Coonrod, "The effects of Design Dk on Microwave Circuit Design," Rogers Corporation Technology Support Hub, 2014.
2. Allen F. Horn, John W. Reynolds, and James C. Ratio, "Conductor Profile Effects on the Propagation Constant of Microstrip Transmission Lines," IMS Microwave Theory and Technology Symposium, 2010.
3. John Coonrod, "What RF Circuit Designers Need to Know About Dk, Part 1 and Part 2," Rogers Corporation Technology Support Hub, Coonrod's Corner videos, November 2015.
4. John Coonrod, "An Overview of Glass weave Impact on Millimeter-Wave PCB Performance," Rogers Corporation Technology Support Hub, October 2018.

Rogers' Laminates: Paving the way for tomorrow's Autonomous Vehicles

Autonomous "self-driving" vehicles are heading our way guided by a variety of sensors, such as short and long range radar, LIDAR, ultrasound and camera. Vehicles will be connected by vehicle-to-everything (V2X) technology. The electronic systems in autonomous vehicles will have high-performance RF antennas. Both radar and RF communication antennas will depend on performance possible with circuit materials from Rogers Corporation.

High-performance circuit laminates, such as RO3000® and RO4000® series materials, are already well established for radar antennas in automotive collision-avoidance radar systems at 24 and 77 GHz. To further enable autonomous driving, higher performance GPS/GNSS and V2X antennas will be needed, which can benefit from the cost-effective high performance of Kappa™ 438 and RO4000 series materials. These antennas and circuits will count on the consistent quality and high performance of circuit materials from Rogers.

Material	Features
RADAR	
RO3003G2™ Laminates	Best in class insertion loss / most stable electrical properties for 77 GHz antennas
RO4830™ Laminates	Cost-effective performance for 77 GHz antennas
RO4835™ Laminates	Stable RF performance for multi-layer 24 GHz antennas
ANTENNA	
RO4000 Series Circuit Materials	Low loss, FR-4 processable and UL 94 V-0 rated materials
Kappa™ 438 Laminates	Higher performance alternative to FR-4

To learn more visit:
www.rogerscorp.com/autonomousdriving

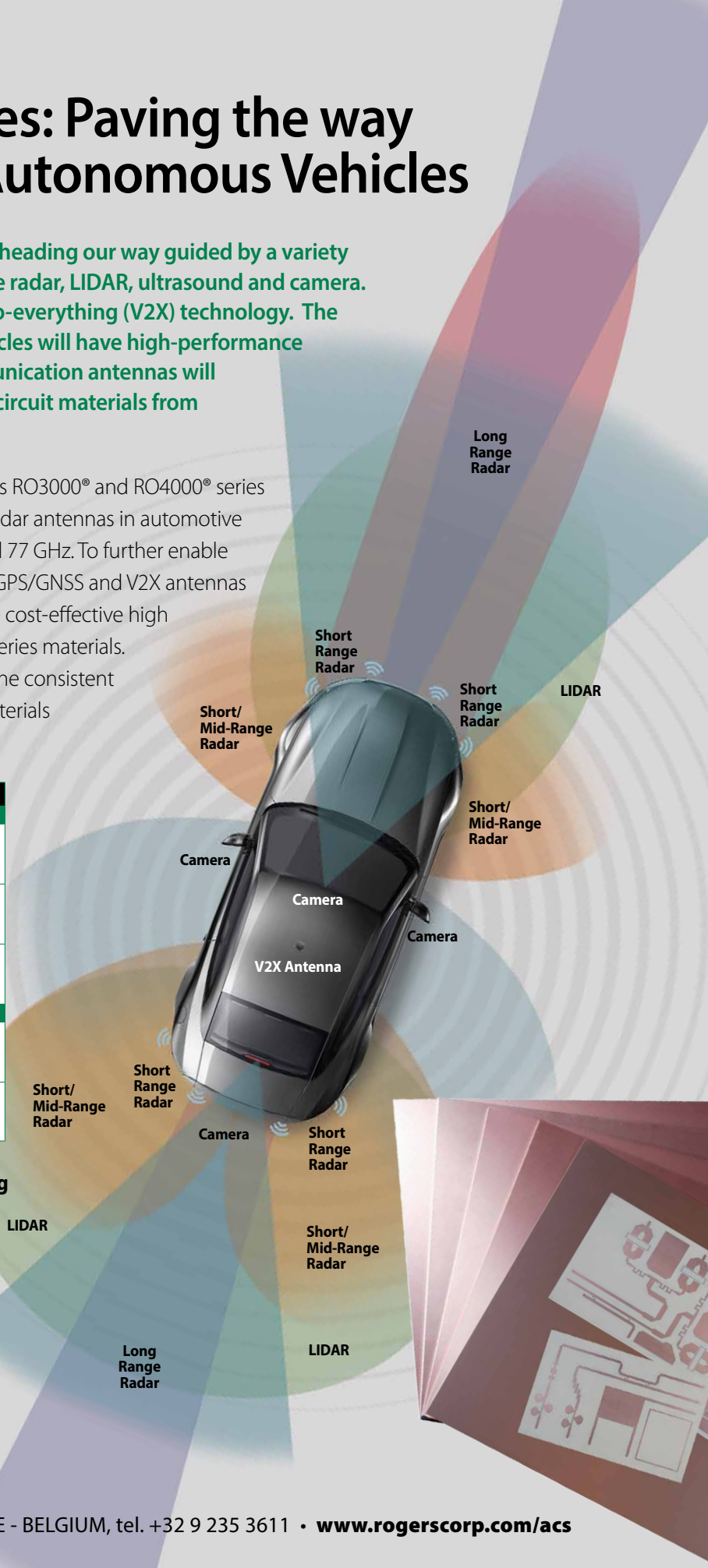

ROGERS CORPORATION

Advanced Connectivity Solutions

USA - AZ, tel. +1 480-961-1382 • EUROPE - BELGIUM, tel. +32 9 235 3611 • **www.rogerscorp.com/acs**